DEVELOPMENT OF ADVANCED MODAL METHODS FOR CALCULATING TRANSIENT THERMAL AND STRUCTURAL RESPONSE

By

Charles J. Camarda

Dissertation submitted to the Faculty of the

Virginia Polytechnic Institute and State University

in partial fulfillment of the requirements for the degree of

Doctor of Philosophy

in

Aerospace Engineering

APPROVED:

Raphael T. Haftka, Chairman

Frederick H. Lutze

Raymond H. Plaut

Liviu Librescu

Rakesh Kapania

September, 1990
Blacksburg, Va.

DEVELOPMENT OF ADVANCED MODAL METHODS FOR CALCULATING TRANSIENT THERMAL AND STRUCTURAL RESPONSE

By

Charles J. Camarda

Committee Chairman: Raphael T. Haftka

Aerospace and Ocean Engineering

(ABSTRACT)

This dissertation evaluates higher-order modal methods for predicting thermal and structural response. More accurate methods or ones which can significantly reduce the size of complex, transient thermal and structural problems are desirable for analysis and are required for synthesis of real structures subjected to thermal and mechanical loading. A unified method is presented for deriving successively higher-order modal solutions related to previously-developed, lower-order methods such as the mode-displacement and mode-acceleration methods. A new method, called the force-derivative method, is used to obtain higher-order modal solutions for both uncoupled (proportionally-damped) structural problems as well as thermal problems and coupled (non-proportionally damped) structural problems. The new method is called the force-derivative method because, analogous to the mode-acceleration method, it

produces a term that depends on the forcing function and additional terms that depend on the time derivatives of the forcing function.

The accuracy and convergence history of various modal methods are compared for several example problems, both structural and thermal. The example problems include the case of proportional damping for: a cantilevered beam subjected to a quintic time-varying tip load and a unit step tip load and a multispan beam subjected to both uniform and discrete quintic time-varying loads. Examples of non-proportional damping include a simple two-degree-of-freedom spring-mass system with discrete viscous dampers subjected to a sinusoidally varying load and a multispan beam with discrete viscous dampers subjected to a uniform, quintic time-varying load. The last example studied is a transient thermal problem of a rod subjected to a linearly-varying, tip heat load.

The higher-order modal methods are shown to converge to an accurate response using fewer eigenmodes than lower-order modal methods. The force-derivative method is very effective in representing the response of the important, but otherwise neglected, higher modes for structural problems in which there are a large number of closely-spaced frequencies (e.g., a multispan beam or a large area truss-type structure). However, for response times close to discontinuities in the forcing function and/or its derivatives, the mode-acceleration or force-derivative methods must include appropriate jump conditions or additional modes to insure accuracy. The higher-order modal methods are also effective in solving transient thermal problems efficiently.

Acknowledgements

I wish to extend my sincere gratitude to my advisor, Dr. Raphael T. Haftka, for his insightful guidance throughout my research and studies, his persistence, perserverance and constant concern and of course, his much valued friendship.

I would also like to express my appreciation to Dr. Howard M. Adelman, my colleague and good friend, for his support and advice during the course of my work.

I would like to include my special thanks to another colleague and friend, Mr. Michael Riley, for his patience and help in computer programming.

I would also like to thank Dr. Jim Starnes for his careful review of this manuscript, Mr. David McGowan for his careful inspection and verification of the results and Mrs. Cheryl W. Winstead for her assistance in the careful preparation of the final document..

In addition, I would like to express my gratitude to the National Aeronautics and Space Administration for allowing me this opportunity to advance my education.

I would also like to thank the members of my committee: Dr. Frederick H. Lutze, Dr. Raymond H. Plaut, Dr. Liviu Librescu, and Dr. Rakesh Kapania.

Dedication

This work is dedicated to my daughter, Chelsea Elise, who is, and will remain, the motivating force in my life and to my parents and family who have stood by me with love and support.

Table of Contents

List of Figures

List of Tables

SYMBOLS

C	damping matrix
E	modulus of elasticity
e	spatial error norm (eq. (45))
I	moment of inertia
K	stiffness matrix
K_1, K_2	spring stiffnesses (see fig. 16)
$\bar{K}$	generalized stiffness matrix, conductance matrix
L	beam length
M	mass matrix, moment
M_1, M_2	discrete masses (see fig. 16)
$\bar{M}$	generalized mass matrix, capacitance matrix
m	subset of total number of degrees-of-freedom
n	total number of degrees-of-freedom
Q	force vector
$\bar{Q}$	generalized force or thermal load vector

q	modal coordinates of the second-order system
r_i	frequency ratio ω_f/ω_i
S	shear force
T	normalized time ($T = \omega_0 t$), temperature vector
t	time
u	displacement
x	coordinate direction
Y	generalized displacement or temperature vector
Z	modal coordinates of the first-order system

Greek

α	ratio of spring stiffnesses (K_1/K_2, see fig. 16)
α_i	ith damped eigenvalue (eqs. (3) and (4))
$[\alpha]$	matrix of damped eigenvalues
Φ_i	ith damped eigenvector
$[\Phi]$	matrix of damped eigenvectors
ϕ_i	ith normal eigenvector (eq. (27))
ε	time-integrated error norm defined in eq. (46)
Ω^2	matrix of frequencies squared (eq. (30))
ω_f	forcing frequency

ω_f forcing frequency

ω_i ith circular natural frequency

ω_0 normalizing frequency $\omega_0 = \sqrt{\frac{EI}{\rho AL^4}}$

ω_{di} ith circular frequency of the damped free vibration

Λ matrix of damping coefficients (eq. (30))

ρ density

τ dummy variable of integration, temporal integral limit (eq. (46))

ζ_i ith modal viscous damping factor

$\mu(t)$ unit step function

Subscripts

o initial

Superscripts

$(\dot{})$ $(\ddot{})$ differentiation with respect to time, once and twice, respectively

a approximate

i raised to ith power

(i) ith derivative with respect to time

T	transpose
^	matrix of reduced number of eigenvectors or eigenvalues or reduced number of modal coordinates

Chapter 1

Introduction

Transient thermal and structural analysis of complicated engineering problems which are modeled as discrete multidegree-of-freedom systems often require the solution of very large systems of equations. The accurate solution of very large systems of coupled differential equations may be difficult and computationally expensive. In addition to calculating the transient response, optimization of the structure under transient thermal and mechanical loading may be necessary. Automated structural design requires numerous solutions of the coupled system of equations to assess the effects of changes in design parameters on response quantities and constraint boundaries. Since the problem is transient, continuous constraint boundaries in time have to be approximated, often requiring many discrete times to be used to approximate the constraint boundaries and ensure that the critical times when the maximum response occurs are properly represented. Automated

design of even moderate-size problems can become intractable when designing for transient loading conditions. Hence, reducing the size of such systems is highly desirable from the standpoint of increased computational efficiency. Some of the many methods for reducing the size of discrete multi-degree-of-freedom structural dynamic systems include mass condensation methods (e.g., refs. 1 to 7) and reduced basis methods (e.g., refs. 8 to 15).

The mass condensation methods typically reduce the size of the dynamic system of equations by condensing out less-important degrees of freedom from the problem. One of the most popular methods, proposed by Guyan (ref. 1), assumes the relationship between the dependent and independent degrees of freedom can be determined by the static relationship between them. Other mass condensation methods either approximate a relationship between dependent and independent degrees of freedom of the dynamic system (ref. 7) or solve exactly for this dynamic relationship (ref. 3). To achieve reasonably accurate results, the set of dependent degrees-of-freedom must be chosen carefully or some of the lower frequencies in the eigenspectrum may be lost. It was also shown in reference 7 that large errors can occur when Guyan reduction is used to expand the mode shapes and calculate forces. Modified mass-condensation methods have been developed to help reduce these deficiencies (refs. 3, 6, and 7). An attempt to extend the Guyan reduction method to transient thermal analysis (ref. 16) resulted in the conclusion that a crude thermal finite-element model (having fewer degrees of freedom than the model reduced using Guyan

reduction) produced results as good as or, in most cases, better than those obtained using Guyan reduction.

The reduced basis methods, on the other hand, use an expansion theorem (ref. 17, pp. 90-91) and a reduced set or subset of linearly independent basis vectors to approximate the transient response. These methods use either a truncated set of complete basis vectors (e.g., eigenmodes (ref. 18), Ritz vectors (ref. 8), or Lanczos vectors (ref. 19)) or a combination of basis vectors (e.g., eigenmodes and Ritz vectors (ref. 14). When a reduced basis method is based on the eigenmodes of the system, the method is referred to as a modal method. One of the first reported uses of eigenmodes to reduce the size of a problem and calculate the dynamic response of an elastic structure was by Biot and Bisplinghoff (ref. 18). In that classic paper, the authors recognized that the transient, linear response of structures can be calculated by a superposition of the natural oscillations or modes since the eigenmodes are orthogonal and linearly independent and form a complete set (this method is herein referred to as the mode-displacement method (MDM)). In addition, for linear dynamic problems without damping or for proportionally-damped problems, the equations of motion of a multi-degree-of-freedom system uncouple and can be solved individually as single-degree-of-freedom systems.

The usefulness of any reduced-basis or mode-superposition method lies in its ability to predict accurately the transient response using only a small number of basis vectors or modes. The need for only a small number of basis vectors for an accurate response is

especially well-suited for modal methods, where it is computationally expensive to calculate the eigenvectors or modes of large systems as compared to other, less expensive reduced basis methods, which use Lanczos vectors (ref. 19) or Ritz vectors (ref. 14). Toward this end, the MDM has proven useful in calculating transient structural displacements for most dynamic structural problems, using only a small percentage of the lower frequency mode shapes.

The MDM can be considered to be a generalization of a Fourier series approximation. It is well known that Fourier series representation of discontinuous functions converge slowly, and that the derivatives of the series may not converge at all. This type of convergence problem is known as the Gibbs phenomenon (ref. 20). Hence, the MDM can be expected to converge slowly when the applied loads exhibit discontinuities in time or space. This slow convergence is exhibited in the transient response problem of a string with a point load (ref. 21), and other examples (e.g., refs. 22 and 23). The MDM is also less accurate in predicting transient stresses (refs. 9 and 24) and, hence, requires more modes to obtain converged accurate stresses. This decreased accuracy in predicting stresses is understandable since the stresses are related to the spatial derivatives of the displacement vector and, hence, errors in the displacements become magnified upon differentiation. In addition, some structural problems which have closely-spaced natural frequencies, such as large area space structures or multispan beams, experience very slow convergence and require a large

number of modes to predict even the displacement response accurately.

The mode-acceleration method (MAM) was developed as a means to improve the convergence of the MDM. The origin of the method is attributed to Williams (ref. 25), but as pointed out by de Veubeke (ref. 9), the original concept was stated by Lord Rayleigh (ref. 26) as early as 1877. Lord Rayleigh noticed that when the periods of the forces operating on a system are long relative to the free vibration periods of the system, the inertial forces of the system can be neglected. The MAM was popularized by Craig (ref. 27) in 1981 and put into a more familiar form. The MAM improves the low-frequency or pseudo-static response convergence because it incorporates, as a separate term, the pseudo-static response in the solution which approximates, to some degree, the flexibility of the higher modes which are neglected in the modal summation. Maddox (ref. 24) indicates an improved accuracy in dynamic force calculations using a MAM-type approach as compared to the MDM approach. Hansteen and Bell (ref. 28) indicate that the inaccuracies of modal truncation in the MDM can be caused by components of the load which are orthogonal to the eigenmodes included in the solution and show that Maddox's proposal is equivalent to the inclusion of an approximate expression for these components of the load. Anagnostopoulos (ref. 29) indicates deficiencies in both the MDM and MAM in calculating forces and stresses in offshore structures when subjected to earthquake-type loading. Leger and Wilson (ref. 30) compare the numerical efficiency of several forms of the MAM as

presented in references 28 and 29. An in-depth comparison of the MDM and MAM methods (ref. 11) indicates that the MAM converges to an accurate solution with fewer modes than the MDM. This study includes a comparison of the effect of proportional damping level and load frequency on the relative accuracy of the response using the MDM and MAM methods.

Attempts at using mode-superposition methods to solve transient, linear thermal problems (refs. 31 to 35) have been unsuccessful because thermal problems exhibit a wide spectrum response where very high frequencies are excited and, hence, a prohibitively large number of "thermal modes" are necessary for an accurate solution. The use of "thermal modes" was first suggested as a solution to transient thermal problems by Biot in reference 36. In that paper, Biot develops an analogous MDM solution and also includes what is analogous to a MAM solution for a plate with one edge insulated and the other edge suddenly brought to constant temperature.

The work of Ramberg (ref. 37) reveals that the MAM can be derived from the MDM by integrating the convolution integral portion of the solution by parts once with respect to time. Leung (ref. 12) improves the convergence of the MAM for undamped systems by integrating the convolution integral several more times. A similar method for developing highly convergent modal solutions to linear dynamic structural problems was suggested by Likhoded (ref. 38), which the author calls "multiple extractions of the pseudo-static component". Likhoded presents a recursive technique for developing higher-order or faster-convergent modal solutions.

Borino and Muscolino (ref. 39) developed a modal method, called the dynamic-correction method (DCM), which separates the homogenuous and complementary solutions of the transient response. The DCM assumes that the transient response at time, t, can be considered as the sum of a pseudo-static response or particular solution, which depends on the load at time, t, plus a dynamic correction which takes into account the dynamic solution due to the loads from the initial time to time t.

The present study extends the work of Leung (ref. 12) by developing a unified method (refs. 13 and 40) for deriving higher-order modal methods which are general in that they: (1) are easy to implement into existing computer programs, (2) can represent proportional as well as non-proportional damping, and (3) can be extended to solve transient, linear heat transfer problems. The newly developed method is called the force-derivative method (FDM) because, analogous to the MAM, the FDM produces a term which depends on the forcing function and additional terms which depend on the time-derivatives of the forcing function (ref. 13). These additional terms produce successively higher-order approximations to the contributions of the higher modes which are neglected in the modal summation.

The effects of various factors on the rate of convergence or accuracy of the various modal summation methods is investigated. These factors include: the differentiability of the forcing function, the frequency of the forcing function, the level of damping, and the time at which the response is calculated. The forcing functions were

chosen to illustrate the effect of a temporally continuous forcing function which has continuous higher derivatives, a discontinuous forcing function (a unit step function), a spatially continuous loading distribution, and a spatially discontinuous loading. Structural problems include both proportional and non-proportional damping as well as the effect of discrete dampers. A quintic function of time was selected to illustrate what happens when the force or one of its derivatives vanish at some point in time. The convergence for a sinusoidal forcing function is also studied.

A series of numerical examples has been selected to illustrate the adequacy and/or inadequacy of each method. The examples, which assume proportional damping, are: (1) a uniform cantilevered beam subject to a quintic time-varying tip load, and a unit step tip load and (2) a multispan beam (10 equal-length spans) subjected to both uniform and discretely applied, quintic time varying loads. Examples assuming non-proportional damping include: (1) a simple two-degree-of-freedom spring-mass system with discrete viscous dampers subjected to a sinusoidally varying load on one of the masses, and (2) a multispan beam with discrete viscous dampers subjected to a discrete, linearly-varying load. In addition, the suitability of using higher-order modal methods to solve transient, linear heat transfer problems was investigated. The last problem studied is a rod heated at one end by either a step tip heat load or a linear time-varying heat load while the other end is maintained at a uniform temperature.

A method for developing higher-order modal methods which mathematically unifies previously developed improved modal methods (refs. 10 to 12, 38, and 39) is presented in Chapter 2. Methods for solving proportionally and non-proportionally damped systems of equations using both damped and undamped eigenmodes are presented. The first-order, damped-mode formulation of the equations of motion is especially suited for solving transient heat transfer problems. Two different error norms are used to evaluate the various methods and are presented in Chapter 3. Analytical results are divided into two separate chapters, one for Structural Analysis (Chapter 4) and another for Thermal Analysis (Chapter 5). A summary and conclusions are given in Chapter 6.

Chapter 2

Unified Derivation of Modal Methods

As mentioned in the introduction, there have been many various modal summation methods and forms of implementation of such methods presented in the literature (e.g., refs. 3, 9, 10-12, 14, 18, 24, 25, 28, 29-31, 36, 38, and 39). The present chapter will describe a unified method for deriving the simplest or zeroth-order form of the modal summation methods, the mode-displacement method (MDM). The method will be shown to be useful for deriving higher-order methods such as the mode-acceleration method (MAM) (which will be shown to be a first-order method). This unified method, which is herein called the force-derivative method (FDM), can be developed in two forms, a first-order or damped-mode formulation which operates on the equations of motion in first-order form and a second-order or natural-mode formulation which operates on the equations of motion which are in a second-order form. The former

uses the damped system eigenvalues and eigenvectors, whereas the latter uses the natural modes and eigenvalues of the system. In addition, alternate forms of the above-mentioned formulations are presented which are easier to implement into existing computer programs.

2.1 First-Order or Damped-Mode Formulation

The equations of motion, in matrix form, of an n-degrees-of-freedom system, together with the initial conditions, are given by

$$M\ddot{u} + C\dot{u} + K u = Q(t) \qquad (1)$$

$$u(0) = u_0, \quad \dot{u}(0) = \dot{u}_0$$

where M, C, and K are the mass, damping, and stiffness matrices of the system; u and Q are the displacement and load vectors, respectively, and a dot denotes differentiation with respect to time.

Transforming eq. (1) into first-order form results in the following system of equations:

$$\bar{M}\dot{Y} + \bar{K}\,Y = \bar{Q} \qquad Y(0) = Y_o \qquad (2)$$

where

$$Y = \begin{Bmatrix} \dot{u} \\ u \end{Bmatrix}, \quad \bar{K} = \begin{bmatrix} -M & 0 \\ 0 & K \end{bmatrix}, \quad \bar{M} = \begin{bmatrix} 0 & M \\ M & C \end{bmatrix}$$

and

$$\bar{Q} = \begin{Bmatrix} 0 \\ Q \end{Bmatrix} \quad , \quad Y_o = \begin{Bmatrix} \dot{u}_o \\ u_o \end{Bmatrix}$$

Assuming a solution to the homogeneous form of eq. (2) as:

$$Y(t) = e^{\alpha_r t}\Phi_r \qquad (3)$$

results in an eigenvalue problem

$$\alpha_r \bar{M}\,\Phi_r + \bar{K}\,\Phi_r = 0. \qquad (4)$$

The eigenvectors (Φ_r) are normalized such that

$$\Phi_r^T \bar{M} \Phi_r = 1.0$$

and then (5)

$$\Phi_r^T \bar{K} \Phi_r = -\alpha_r$$

Equation (5) can also be written in matrix form as

$$[\Phi]^T \bar{M} [\Phi] = [I] \quad \text{and} \quad [\Phi]^T \bar{K} [\Phi] = -[\alpha]$$

where $[\Phi]$ is a 2n-by-2n modal matrix with its ith column equal to Φ_r and $[\alpha]$ is a diagonal matrix consisting of the α_r's.

A solution to eq. (2) is assumed in the form of the following modal summation

$$Y(t) = \sum_{r=1}^{2n} \Phi_r Z_r(t) \qquad (6)$$

Substituting eq. (6) into eq. (2) with premultiplication by Φ_r^T results in the following, uncoupled, system of equations:

$$\dot{Z}_r - \alpha_r Z_r = \Phi_r^T \bar{Q} \qquad (7)$$

$$Z_r(0) = Z_{ro} = \Phi_r^T \bar{M} Y_o$$

The solution to eq. (7) is

$$Z_r(t) = Z_{ro}\, e^{\alpha_r t} + \int_0^t e^{\alpha_r(t-\tau)} \Phi_r^T \bar{Q}(\tau) d\tau \qquad (8)$$

Hence, the solution of eq. (2) becomes

$$Y(t) = \sum_{r=1}^{2n} \Phi_r \left[Z_{ro}\, e^{\alpha_r t} + \int_0^t e^{\alpha_r(t-\tau)} F_r(\tau) d\tau \right] \qquad (9)$$

where

$$F_r(\tau) = \Phi_r^T \bar{Q}(\tau)$$

If the forcing function has continuous derivatives, the convolution integral of eq. (9) can be integrated by parts to produce higher-order

modal methods (ref. 13). For example, if it is integrated by parts once, the following expression results

$$Y(t) = \sum_{r=1}^{2n} \Phi_r \left[Z_{ro} + \frac{F_r(0)}{\alpha_r} \right] e^{\alpha_r t} - \frac{\Phi_r F_r(t)}{\alpha_r}$$

$$+ \frac{\Phi_r}{\alpha_r} \int_0^t e^{\alpha_r (t-\tau)} \cdot F_r(\tau) d\tau) \qquad (10)$$

If all the modes are used in the second-to-last term in eq. (10), this term can be written as

$$\sum_{r=1}^{2n} -\Phi_r \frac{1}{\alpha_r} F_r(t) = -[\Phi] \left[\frac{1}{\alpha} \right] [\Phi]^T \bar{Q}(t) = \bar{K}^{-1} \bar{Q}(t) \qquad (11a)$$

since from eq. (5)

$$\left[[\Phi]^T \bar{K} [\Phi] \right]^{-1} = -[\alpha]^{-1} \quad \text{or} \quad [\Phi]^{-1} \bar{K}^{-1} [\Phi]^{-T} = -\left[\frac{1}{\alpha} \right] \qquad (11b)$$

Pre- and post-multiplying eq. (11b) by $[\Phi]$ and $[\Phi]^T$, respectively, leads to

$$\bar{K}^{-1} = -[\Phi] \left[\frac{1}{\alpha} \right] [\Phi]^T \qquad (11c)$$

where $\left[\frac{1}{\alpha} \right]$ is a diagonal matrix whose elements are $\frac{1}{\alpha_r}$.

If equation (11) is substituted into equation (10), the resulting expression can be written as

$$Y(t) = \sum_{r=1}^{2n} \left\{ \Phi_r \left[Z_{ro} + \frac{F_r(0)}{\alpha_r} \right] e^{\alpha_r t} + \frac{\Phi_r}{\alpha_r} \int_0^t e^{\alpha_r (t-\tau)} \cdot F_r(\tau) d\tau \right\}$$

$$+ \bar{K}^{-1} \bar{Q}(t) \qquad (12)$$

If the forcing function has continuous derivatives up to order N-1 (C^{N-1} continuity), the convolution integral of eq. (9) can be integrated by parts N times, resulting in the following expression:

$$Y(t) = \sum_{r=1}^{2n} \left\{ \Phi_r \left[Z_{ro} + \sum_{i=1}^{N} \frac{F_r^{(i-1)}(0)}{\alpha_r^i} \right] e^{\alpha_r t} + \frac{\Phi_r}{\alpha_r^N} \int_0^t e^{\alpha_r (t-\tau)} F_r^{(N)}(\tau) d\tau \right.$$

$$\left. - \sum_{i=1}^{N} \frac{\Phi_r F_r^{(i-1)}(t)}{\alpha_r^i} \right\} \qquad (13)$$

where the superscript (i-1) denotes the (i-1)th derivative with respect to time.

If all the modes are used in the last N-terms of eq. (13), these terms can be represented as functions of $\bar{M}$ and $\bar{K}$ (ref. 40) as follows

$$Y(t) = \sum_{r=1}^{2n} \left\{ \Phi_r \left[Z_{ro} + \sum_{i=1}^{N} \frac{F_r^{(i-1)}(0)}{\alpha_r^i} \right] e^{\alpha_r t} + \frac{\Phi_r}{\alpha_r^N} \int_0^t e^{\alpha_r (t-\tau)} F_r^{(N)}(\tau) d\tau \right\}$$

$$+ \sum_{i=1}^{N} \left(- \bar{K}^{-1} \bar{M} \right)^{i-1} \bar{K}^{-1} \bar{Q}^{(i-1)}(t) \qquad (14)$$

2.2 Alternate Damped-Mode Formulation

Equations 8 to 14 are analogous to those presented in reference 13. However, the present expressions solve a first-order system of equations, using the damped modes, Φ_r, to decouple a non-proportionally damped system (the damping matrix is not a linear function of the mass and stiffness matrices). The first-order system of equations is twice as large as the second-order system. Equation 14 represents a means for developing higher-order modal methods than either the MDM or MAM. This method is called the force-derivative method (FDM) (refs. 13 and 40) because it produces terms which are related to the forcing function and its time derivatives.

Equation 2 can also be considered to represent a heat conduction problem where, for that problem, $\bar{M}$ represents the capacitance matrix, $\bar{K}$ represents the conductance matrix, $\bar{Q}$ represents the thermal load vector, and Y is the vector of nodal temperatures.

The MDM uses a subset, m ($m < 2n$), of the eigenmodes to reduce the size of the problem and solves for Z_r using eq. (8) (or simply by numerically integrating eq. (7)) and substitutes these values into a reduced modal summation in eq. (6) to approximate the response, Y(t). The MDM can be classified as a zeroth-order method because it is equivalent to using the FDM (eq. (14)) with $N = 0$. An analogous form of the MAM uses eq. (12), and a reduced modal summation to approximate Y(t) and can be classified as a first-order method ($N = 1$ in eq. (14)). The FDM uses eq. (14) with $N > 1$. (Results presented in this study assume $N = 4$ when referring to the FDM method). Reference 13 showed that the expressions obtained using the FDM offer improved approximations to the contributions of higher, neglected, modes for several structural problems.

The FDM (eq. (14)) can be derived using an approach similar to that used in reference 39 which results in a form which is more suitable for inclusion into existing thermal and structural analysis codes. A numerical approach can be derived, similar to that presented in reference 39, which approximates the forcing function as a piecewise differentiable polynomial and which numerically integrates the reduced system of equations (eq. (8)). For example, assuming the

forcing function is C^0 continuous; eq. (7) could be rearranged as shown

$$Z_r(t) = -\frac{1}{\alpha_r}\Phi_r^T \bar{Q}(t) + \frac{1}{\alpha_r}\dot{Z}_r(t) \tag{16}$$

Using eqs. (6) and (11), and (16), the response can be written as

$$Y(t) = \bar{K}^{-1}\bar{Q}(t) + \sum_{r=1}^{2n}\Phi_r\frac{1}{\alpha_r}\dot{Z}_r(t) \tag{17}$$

The last term can be evaluated using eq. (8) and Leibnitz's rule for differentiation of an integral to produce the following:

$$\dot{Z}_r(t) = \Phi_r^T\bar{Q}(t) + \alpha_r Z_{ro}\, e^{\alpha_r t} + \alpha_r\int_0^t e^{\alpha_r(t-\tau)}\Phi_r^T\bar{Q}(\tau)d\tau \tag{18}$$

Y(t) can be approximated using only a subset of the modes for the last term in eq. (17), and using eqs. (8) and (18), eq. (17) becomes

$$Y(t) \cong \left(\bar{K}^{-1} + \hat{\Phi}\,\hat{\alpha}^{-1}\hat{\Phi}^T\right)\bar{Q}(t) + \hat{\Phi}\hat{Z}(t) \tag{19}$$

where the ^ denotes a reduced set of modes ($m < 2n$), $\hat{\alpha}^{-1}$ represents a diagonal matrix consisting of a reduced number of eigenvalues α_r^{-1}, and $Z(t)$ can be calculated by either numerically integrating eq. (7) or by using an analytic expression, when applicable, for a given forcing function. Equation 19 is an alternate form of the MAM.

If the forcing function can be assumed to be C^1 differentiable, eq. (7) can be differentiated once with respect to time and re-arranged as shown below:

$$\dot{Z}_r(t) = -\frac{1}{\alpha_r}\Phi_r^T \dot{\bar{Q}}(t) + \frac{1}{\alpha_r}\ddot{Z}_r(t) \tag{20}$$

Re-arranging eq. (7) and substituting for $\dot{Z}_r$ from eq. (20) results in

$$Z_r(t) = -\frac{1}{\alpha_r}\Phi_r^T \bar{Q}(t) - \frac{1}{\alpha_r^2}\Phi_r^T \dot{\bar{Q}}(t) + \frac{1}{\alpha_r^2}\ddot{Z}_r(t) \tag{21}$$

Using eqs. (5) and (6), the response can be written as

$$Y(t) = \bar{K}^{-1}\bar{Q}(t) - \bar{K}^{-1}\bar{M}\bar{K}^{-1}\dot{\bar{Q}}(t) + \sum_{r=1}^{2n}\Phi_r\frac{1}{\alpha_r^2}\ddot{Z}_r(t) \tag{22}$$

where the second term in eq. (21) is determined using eq. (11) and it is assumed that the modes can be normalized as shown by eq. (5).

The last term in eq. (22) can be evaluated using eq. (8) and Leibnitz's rule for differentiation of an integral to produce the following:

$$\ddot{Z}_r(t) = \alpha_r \Phi_r^T \bar{Q}(t) + \Phi_r^T \dot{\bar{Q}}(t) + \alpha_r^2 Z_{ro} e^{\alpha_r t} + \alpha_r^2 \int_0^t e^{\alpha_r (t-\tau)} \Phi_r^T \bar{Q}(\tau) d\tau \qquad (23)$$

Once again, Y(t) can be approximated by using a subset of the modes for the last term in eq. (22), and using eqs. (8) and (23), eq. (22) becomes

$$Y(t) \equiv \left(\bar{K}^{-1} + \hat{\Phi} \hat{\alpha}^{-1} \hat{\Phi}^T \right) Q(t) + \left(\bar{K}^{-1} \bar{M} \bar{K}^{-1} + \hat{\Phi} \hat{\alpha}^{-2} \hat{\Phi}^T \right) \dot{Q}(t) + \hat{\Phi} \hat{\ddot{Z}}(t) \qquad (24)$$

If a C^2 differentiable forcing function is assumed, eq. (7) could be differentiated twice and a procedure, similar to that outlined by eqs. (20) to (24), would produce the following expression:

$$Y(t) \cong \left(\bar{K}^{-1} + \hat{\Phi}\,\hat{\alpha}^{-1}\hat{\Phi}^{T}\right)Q(t) + \left(-\bar{K}^{-1}\bar{M}\bar{K}^{-1} + \hat{\Phi}\,\hat{\alpha}^{-2}\hat{\Phi}^{T}\right)\dot{Q}(t)$$
$$+\left(\bar{K}^{-1}\bar{M}\bar{K}^{-1}\bar{M}\bar{K}^{-1} + \hat{\Phi}\,\hat{\alpha}^{-3}\hat{\Phi}^{T}\right)\ddot{Q}(t) + \hat{\Phi}\hat{Z}(t) \qquad (25)$$

This expression for Y(t) shown by eq. (25) can be expanded, by assuming the forcing function is C^N differentiable, to give

$$Y(t) \cong \sum_{i=1}^{N+1}\left[\left(\left(-\bar{K}^{-1}\bar{M}\right)^{i-1}\bar{K}^{-1} + \hat{\Phi}\,\hat{\alpha}^{-i}\hat{\Phi}^{T}\right)\bar{Q}^{(i-1)}(t)\right] + \hat{\Phi}\hat{Z}(t) \qquad (26)$$

Compared to eq. (14), the alternate formulation of the FDM (eq. (26)) does not require the solution of a convolution-type integral. In addition, the last term of eq. (26) is identical to a mode-displacement solution and, as such, the form of the FDM as given by eq. (26) is more suited for inclusion into existing computer codes.

2.3 Second-Order or Natural-Mode Formulation

Expressions which use the undamped natural modes can be developed in an analogous manner as the damped-mode formulation and result in an expression similar to eqs. (19) and (24) to (26). Beginning with the second-order system of equations (eq. (1)), the undamped or natural modes, ϕ_r, are determined by solving the following eigenvalue problem:

$$K\phi_r = \omega_r^2 M\phi_r \tag{27}$$

where ω_r is the rth circular natural frequency.

The modes are normalized as follows:

$$\phi_r^T M \phi_r = 1.0$$

so that

$$\phi_r^T K \phi_r = \omega_r^2 \tag{28}$$

Hence, the displacement response can be represented as

$$u(t) = \sum_{r=1}^{n} \phi_r q_r(t) \tag{29}$$

Using eq. (29) and premultiplying eq. (1) by ϕ_r^T results in

$$\ddot{q} + \Lambda \dot{q} + \Omega^2 q = [\phi]^T Q(t) \qquad (30)$$

where

$$\Lambda = [\phi]^T C [\phi]$$

and

$$\Omega^2 = [\phi]^T K [\phi]$$

where $[\phi]$ is the matrix of undamped eigenmodes, Ω^2 is a diagonal matrix whose diagonal terms can be represented as $\Omega^2_{ii} = \omega_i^2$ and, for proportional damping (where the damping matrix can be represented as a linear combination of the mass and stiffness matrices), Λ is also a diagonal matrix whose diagonal terms can be represented as $\Lambda_{ii} = 2\zeta_i\omega_i$.

Assuming proportional damping and zero initial conditions, the solution to eq. (30) can be written as

$$q_r(t) = \frac{1}{\omega_{dr}} \int_0^t e^{\zeta_r \omega_r (t-\tau)} \sin \omega_{dr}(t-\tau) \phi_r^T Q(\tau)\, d\tau \qquad (31)$$

where

$$\omega_{dr} = \sqrt{\omega_r^2 - (\zeta_r \omega_r)^2}$$

The MAM is equivalent to the FDM of order one (assuming one integration by parts of the convolution integral). This equivalence can be shown by integrating eq. (31) by parts once with respect to time, premultiplying by ϕ_r^T, and substituting into eq. (29). This results in:

$$u(t) \equiv \sum_{r=1}^{m} \phi_r q_r(t)$$

$$= \sum_{r=1}^{m} \phi_r \left[\frac{-\phi_r^T Q(0)}{\omega_r^2} e^{-\zeta_r \omega_r t} \left\{ \frac{\zeta_r \omega_r}{\omega_{dr}} \sin(\omega_{dr} t) + \cos(\omega_{dr} t) \right\} \right.$$

$$\left. + \frac{1}{\omega_r^2} \phi_r^T Q(t) \right) \qquad (32)$$

$$\left. + \int_0^t \frac{-\phi_r^T \dot{Q}(\tau)}{\omega_r^2} e^{-\zeta_r \omega_r (t-\tau)} \left\{ \frac{\zeta_r \omega_r}{\omega_{dr}} \sin \omega_{dr}(t-\tau) + \cos \omega_{dr}(t-\tau) \right\} d\tau \right]$$

If all the modes are used in the second-to-last term of eq. (32), it can be written as

$$u(t) \cong K^{-1} Q(t) + \sum_{r=1}^{m} \phi_r \left[\frac{-\phi_r^T Q(0)}{\omega_r^2} e^{-\zeta_r \omega_r t} \left\{ \frac{\zeta_r \omega_r}{\omega_{dr}} \sin(\omega_{dr} t) + \cos(\omega_{dr} t) \right\} \right. \tag{33}$$

$$\left. + \int_0^t \frac{-\phi_r^T \dot{Q}(\tau)}{\omega_r^2} e^{-\zeta_r \omega_r (t-\tau)} \left\{ \frac{\zeta_r \omega_r}{\omega_{dr}} \sin\omega_{dr}(t-\tau) + \cos\omega_{dr}(t-\tau) \right\} d\tau \right]$$

Equation (33) can be shown to be equivalent to the MAM (ref. 11), the expression of which is shown below:

$$u(t) \cong K^{-1} Q(t) - \sum_{r=1}^{m} \phi_r \left\{ \frac{2\zeta_r}{\omega_r} \dot{q}(t) + \frac{1}{\omega_r^2} \ddot{q}(t) \right\} \tag{34}$$

Using Leibnitz's rule for differentiation of an integral and differentiating eq. (31) with respect to time twice gives

$$\dot{q}_r(t) = \frac{1}{\omega_{dr}} \int_0^t e^{-\zeta_r \omega_r (t-\tau)} \left\{ -\zeta_r \omega_r \sin\omega_{dr}(t-\tau) + \omega_{dr} \cos\omega_{dr}(t-\tau) \right\} \phi_r^T Q(\tau)\, d\tau$$

and (35)

$$\ddot{q}_r(t) = \phi_r^T Q(t) + \frac{1}{\omega_{dr}} \int_0^t e^{-\zeta_r \omega_r (t-\tau)} \times$$

$$\left\{ (2(\zeta_r \omega_r)^2 - \omega_r^2) \sin\omega_{dr}(t-\tau) + 2\zeta_r \omega_r \omega_{dr} \cos\omega_{dr}(t-\tau) \right\} \phi_r^T Q(\tau) d\tau$$

Substituting eqs. (35) into eq. (34) and simplifying, results in

$$u(t) \equiv \overset{-1}{K} Q(t) + \sum_{r=1}^{m} \left(-\phi_r \frac{1}{\omega_r^2} \phi_r^T Q(t) + \phi_r q_r(t) \right) \qquad (36)$$

Integrating the convolution integral expression for $q_r(t)$ with respect to time once, as was done earlier (eq. (32)), it is easy to verify that the MAM (eq. (36)) is equivalent to the FDM of order one (eq. (33)). This equivalence was also shown in references 13 and 37.

2.4 *Alternate Natural-Mode Formulation*

An alternate natural-mode formulation is developed in a similar manner as the alternate formulation of the first-order or damped-mode formulation of Section 2.2. This alternate form is well-suited for inclusion into existing computer codes. Assuming the forcing function is C^2 differentiable, eq. (30) can be differentiated twice and substituted back into eq. (30) to produce the following expression:

$$q(t) = \Omega^{-2}[\phi]^T Q(t) - \Omega^{-2}\Lambda\Omega^{-2}[\phi]^T \dot{Q} + \left[\Omega^{-2}\Lambda\Omega^{-2}\Lambda\Omega^{-2} - \Omega^{-2}\Omega^{-2}\right]\phi^T \ddot{Q}$$
$$+\left[\Omega^{-2}\Omega^{-2}\Lambda - \Omega^{-2}\Lambda\Omega^{-2}\Lambda\Omega^{-2}\Lambda + \Omega^{-2}\Lambda\Omega^{-2}\right] q^{(3)}(t)$$
$$+\left[\Omega^{-2}\Omega^{-2} - \Omega^{-2}\Lambda\Omega^{-2}\Lambda\Omega^{-2}\right] q^{(4)}(t) \qquad (37)$$

If eq. (31) is differentiated with respect to t and the expressions for $q^{(3)}$ and $q^{(4)}$ are substituted into eq. (37), the entire expression reduces to the following:

$$u(t) \cong \left(K^{-1} - \hat{\phi}\,\hat{\Omega}^{-2}\hat{\phi}^{T}\right)Q(t) - \left(K^{-1}CK^{-1} - \hat{\phi}\,\hat{\Omega}^{-2}\hat{\Lambda}\,\hat{\Omega}^{-2}\hat{\phi}^{T}\right)\dot{Q}(t)$$

$$- \left[\left(K^{-1}MK^{-1} - K^{-1}CK^{-1}CK^{-1}\right) - \left(\hat{\phi}\,\hat{\Omega}^{-2}\hat{\Omega}^{-2}\hat{\phi}^{T} - \hat{\phi}\,\hat{\Omega}^{-2}\hat{\Lambda}\,\hat{\Omega}^{-2}\hat{\Lambda}\,\hat{\Omega}^{-2}\hat{\phi}^{T}\right)\right]\ddot{Q}(t)$$

$$+ \hat{\phi}\,\hat{q}(t) \qquad (38)$$

Equation (38) agrees with results presented in reference 39 and, as shown in reference 39, is also valid for non-proportionally damped structural systems. Assuming higher-order piecewise differentiable forcing functions, the method above can produce successively higher-order modal methods and, as such, is just another formulation of the FDM.

The expression for an N^{th}-order modal method can be expressed as

$$u(t) \equiv \sum_{r=1}^{N} \left(B_{1,r-1} - \hat{\phi}\, A_{1,r-1} \hat{\phi}^{T} \right)^{(r-1)} Q(t) + \hat{\phi}\, \hat{q}(t) \qquad (39)$$

where

$$B_r = \begin{bmatrix} B_{1,r} \\ B_{2,r} \end{bmatrix} = \begin{bmatrix} -K^{-1} C B_{1,r-1} - K^{-1} M B_{2,r-1} \\ B_{1,r-1} \end{bmatrix}, \quad B_o = \begin{bmatrix} K^{-1} \\ 0 \end{bmatrix}$$

and

$$A_r = \begin{bmatrix} A_{1,r} \\ A_{2,r} \end{bmatrix} = \begin{bmatrix} -\hat{\Omega}^{-2} \hat{\Lambda} A_{1,r-1} - \hat{\Omega}^{-2} A_{2,r-1} \\ A_{1,r-1} \end{bmatrix}, \quad A_o = \begin{bmatrix} \hat{\Omega}^{-2} \\ 0 \end{bmatrix}$$

2.5 The Dynamic-Correction Method (DCM)

The dynamic-correction method (DCM), reference 39, assumes a solution to eq. (2) in the form

$$Y(t) = Y_P(t) + Y_C(t) \tag{40}$$

where $Y_P(t)$ is a particular solution of eq. (2) and $Y_C(t)$ is the complementary solution which represents the effects of initial conditions. In modal form, $Y_P(t)$ and $Y_C(t)$ can be represented as

$$Y_P(t) = [\Phi]\, Z_P(t)$$

and (41)

$$Y_C(t) = [\Phi]\, Z_C(t)$$

where $Z_P(t)$ and $Z_C(t)$ are the vectors of the particular and complementary solutions to the modal coordinate equations (eq. (7)).

Using eqs. (6) and (41)

$$Y(t) = [\Phi]\, Z(t) = [\Phi][Z(t) - Z_P(t)] + Y_P(t) \tag{42}$$

The fundamental principle of the DCM is that, if available, an exact particular solution to eqs. (2) and (7) can be used to approximate the response (eq. (40)) using a reduced set of modes as shown below:

$$Y(t) \cong \hat{\Phi}\hat{Z}(t) + \left[Y_P(t) - \hat{\Phi}\,\hat{Z}_P(t) \right] \tag{43}$$

It can also be shown that in the limit as N goes to infinity, two terms in equation (26) can be written as

$$\lim_{N\to\infty} \left\{ -\hat{\Phi} \left[\sum_{i=1}^{N} \hat{\alpha}^{-i} \Phi^T \bar{Q}^{(i-1)}(t) \right] \right\} = \hat{\Phi}\hat{Z}_R(t)$$

and (44)

$$\lim_{N\to\infty} \left\{ \left[\sum_{i=1}^{N} \left(\left(-\bar{K}^{-1}\bar{M} \right)^{i-1} \bar{K}^{-1} \right) \Phi^T \bar{Q}^{(i-1)}(t) \right] \right\} = Y_P(t)$$

Hence, if an infinite number of integrations-by-parts are assumed in the FDM or if the convolution integral vanishes (e.g., for a polynomial forcing function of a lower order than the order of the FDM) the FDM would be equivalent to the DCM of reference 39. Also, if an exact solution to the convolution integrals (eqs. (8), (12), (14), (33), etc.) exists and is used, the response can be calculated without the errors caused by approximating the forcing function.

Chapter 3

Error Norm Definition

It is important to develop reliable error estimates to evaluate or compare, quantitatively, the various modal reduction methods. As mentioned previously, classical modal superposition methods for linear systems use a subset of the lower modes to approximate the transient response. The error estimates used here compare the exact or converged response with an approximation to that response, obtained by using a subset of the eigenmodes. These error norms are not intended to be used to predict, a priori, the number of modes necessary for convergence and, hence, the time for termination of the modal series. The convergence of each method (number of modes versus the accuracy of the transient response) is measured by using one of two relative error norms: a spatial error norm or a time-integrated error norm.

3.1 Spatial Error Norm

The spatial error norm, e, of an approximation to the temperature vector is given by

$$e = \sqrt{\frac{(T - T^a)^T (T - T^a)}{T^T T}} \qquad (45)$$

where T represents a converged solution for the temperature vector and T^a is an approximation which can be based on the first m thermal modes.

3.2 Time-Integrated Error Norm

A time-integrated error norm, similar to that used in reference 39, can be used for the error in displacement u_i and is shown below:

$$\varepsilon_i (\%) = \frac{\int_0^\tau | u_i(t) - u_i^a(t) | \, dt}{\int_0^\tau | u_i(t) | \, dt} \; X \; 100 \qquad (46)$$

where ε_i is the time-integrated error in the ith nodal displacement, $u_i(t)$ is the exact response using all the modes of the system, and $u_i^a(t)$ is the approximate response at node i using a subset of the lower modes. The time, τ, selected as the upper limit of integration was chosen to be $\tau = 16\pi/\omega_f$, where ω_f is the forcing function frequency.

Chapter 4

Structural Analysis

The following sections investigate the effect of various forcing functions, load distributions, and damping levels on the transient response of a uniform cross-section cantilevered beam, a uniform, simply-supported multispan beam, and a spring-mass-damper system. The rate of convergence of each of the methods (MDM, MAM, FDM, and DCM) is expected to depend on the nature of the forcing function, the level of damping and the time at which the response is calculated. Proportional damping, when assumed, is constant for all modes. The forcing functions are selected to investigate the effects of continuous forcing functions with vanishing higher derivatives at various times ($Q(T) = 1000(T^4 - T^5)$), the effect of a discontinuous forcing function representing a unit step at time T = 0 ($Q(T) = \mu(T)$), a spatially discontinuous forcing function, and the effect of a sinusoidal forcing function ($Q(T) = \sin \omega_f T$), where T is the normalized time, $T = \omega_0 t$, and ω_0 is the normalizing frequency, $\omega_0 = \sqrt{\frac{EI}{\rho A L^4}}$. In addition, the effects of non-proportional damping are investigated. It is

assumed that for all forcing functions, Q(T) = 0 for T < 0. Several example problems, described below, are selected to evaluate the accuracy of each method.

The spatial error norm, e (eq. (45)), is used to evaluate the various modal methods. The effectiveness of this error norm in quantifying the global error associated with each of the modal methods is demonstrated for a cantilevered beam problem. The displacement distribution of a cantilevered beam with a quintic varying tip load in time of $Q(T) = 1000(T^4 - T^5)$ lb. at a normalized time T = 0.4 and for $\zeta_i = 0.05$ is shown in figure 1a for each of the various modal methods using only one mode. The value of the spatial error, e, is also listed in the figure. Notice that as the value of the error norm decreases, the distributions approach that of the MDM using 30 modes, as indicated by the solid line. As shown in figure 1a, only one mode is used and for the MDM, e = 0.289 and displacement errors are noticeable. However the MAM, FDM and DCM results, having error norms of e = 0.0407, 0.0008, and 0.001, respectively, are indistinguishable from the converged solution (MDM using 30 modes). Similarly, for the normalized moment distribution (Fig. 1b) the MDM (using the first two modes) has an error e = 0.395, and the MAM, FDM and DCM (all three using only the first mode) have errors of e = 0.1190, 0.0023, and 0.0033, respectively. As shown in figures 1a and 1b, there is a qualitative improvement in the solution (response distribution) as the error norm e decreases in magnitude.

4.1 Proportional Damping

The equations of Chapter 2 are used to study several beam example problems: a cantilevered beam with a tip loading and a multispan beam with uniform and discrete loadings. These problems use analytical expressions for the mode shapes $\phi_r(x)$ (refs. 17 and 41), mode-shape derivatives, and modal coordinates $q_r(t)$ (eq. 29). The use of analytical solutions to calculate the transient response of the modal coordinates, q_r, eliminates the need for numerical integration in time and associated numerical errors. As mentioned in Chapter 2, the MDM and MAM can be considered as the FDM of order zero and one, respectively. The results labeled FDM in the figures, refer to a fourth-order version of the FDM which is obtained assuming the forcing function has derivatives of order four or higher. Modal vectors are calculated assuming 51 equally-spaced points along the length of the beam. The solution formulation used is the second-order or natural-mode formulation (Section 2.3) where the convolution integral portion of the expression (e.g., eq. (33) and ref. 13) is evaluated analytically.

Moment and shear forces were calculated from the following equations:

$$M(x,t) = EI\frac{\partial^2 u(t)}{\partial x^2}$$

and (47)

$$S(x,t) = EI\frac{\partial^3 u(t)}{\partial x^3}$$

For most cases, 30 modes are sufficient for an accurate solution and, hence, 30 modes are used to approximate expressions such as

$$K^{-1} \cong \sum_{r=1}^{30} \phi_r \left(\frac{1}{\omega_r^2}\right) \phi_r^T ,$$

(48)

$$K^{-1} M K^{-1} \cong \sum_{r=1}^{30} \phi_r \left(\frac{1}{\omega_r^4}\right) \phi_r^T \text{ , etc.}$$

The multispan beam examples experience much slower convergence and, hence, for this problem 50 modes are used to represent the exact solution.

4.1.1 Cantilevered Beam with Tip Loading

The first problem studied is a uniform cantilevered beam loaded by a tip loading. The first 30 natural frequencies of the beam are listed in Table 1. The full 30 modes are used in expressions like eq. (48) to represent the converged solution. The beam is subjected to various levels of modal damping (same value for all modes) and a variety of loading conditions.

4.1.1.1 Quintic Time-Varying Load.- For this problem the forcing function is $Q(T) = 1000(T^4 - T^5)$, where T is the normalized value of time. This problem was presented in reference 12 for the case of zero proportional damping in all modes ($\zeta_i = 0$). This forcing function was chosen to evaluate the various higher-order modal methods since the function or one of its derivatives vanishes at various times: $Q(T) = 0$ when $T = 1.0$;

$\dot{Q}(T) = 0$ when $T = 0.8$; $\ddot{Q}(T) = 0$ when $T = 0.6$; $Q^{(3)}(T) = 0$ when $T = 0.4$; and

$Q^{(4)}(T) = 0$ when $T = 0.2$. This fact affects the convergence of the method as will be shown subsequently. The forcing function is plotted as a function of time, from time $T = 0$ to time $T = 1.2$, in figure 2a. The variation of tip displacement as a function of time, for the case of zero damping ($\zeta_i = 0$), is shown if figure 2b. As shown in figure 2b, the tip displacement decreases to a minimum value of about -30.0 in. at 1.1 sec, shortly after the forcing function changes sign at $T = 1.0$ (see fig. 2a). The moment error norm as a function of the number of the modes used in the modal summation is

shown in figure 3 for time T = 1.2 and ζ_i = 0.05 in all the modes. The FDM offers an improvement in accuracy of several orders of magnitude in the error norm over either the MDM or the MAM. The DCM (or in this case the FDM of order six) results in over an order-of-magnitude increase in accuracy over the FDM (of order four). The advantage of using higher-order modal methods (MAM, FDM, or DCM) lies in the ability of those methods to approximate the flexibility of the higher, but neglected, modes with terms which are functions of the stiffness, mass, and damping matrices and the forcing function and, in the case of the FDM and DCM, its derivatives with respect to time (see, for example, eqs. (14), (26), and (39)). The FDM and DCM offer higher-order approximations by using additional terms together with the pseudo-static response ($K^{-1}Q(T)$). For this problem FDM assumes N = 4 in eq. (39) and the DCM assumes N = 6 (hence fourth- and sixth-order, respectively). The moment error norm (using five modes) is plotted as a function of time in figure 4. At T = 1.0, the value of the moment error norm associated with the MDM is equivalent to the MAM value because at time T = 1.0 , Q(T) = 0 and there is no difference between MDM (N=0) and MAM (N=1) (comparing eqs. (29) and (36)) and, hence, the MDM shows a sharp decrease in error at T = 1.0. A similar decrease in error in the MAM error occurs at time T = 0.8, which corresponds to a time when $\dot{Q}(T) = 0$. These narrow regions where there is a sharp increase in solution accuracy can be anticipated a priori from a knowledge of the times at which the zeroes of the forcing function and its derivatives occur.

A comparison of displacement, moment and shear errors for ζ_i = 0 and times T = 0.6 and T = 1.0 are shown in figures 5a and 5b, respectively. The

error associated with the displacements is the lowest, the moment errors are greater, and the shear errors are the largest. The order of accuracy among the displacement, moment, and shear response is expected because the moments and shears are functions of successively higher spatial derivatives of the displacements (ref. 11). When $T = 0.6$ and $\zeta_i = 0$, the MAM and FDM ($N = 4$) are equivalent (fig. 5a) because $\ddot{Q}(T) = 0$. When $T = 1.0$, the MDM and MAM are equivalent (fig. 5b) for reasons mentioned earlier. When $T = 1.0$ and $\zeta_i = 0$, the only difference between the MDM and MAM and the FDM lies in the term $\left(K^{-1} MK - \hat{\phi} \hat{\Omega}^{-2} \hat{\Omega}^{-2} \hat{\phi} \right) \ddot{Q}(T)$ (eq. (38)). The difference between the methods is less at $T = 1.0$ ($Q(T) = 0.$) than at $T = 0.6$ (fig. 5a), where the difference between the methods lies in the term $\left(K^{-1} - \hat{\phi} \hat{\Omega}^{-2} \hat{\phi}^T \right) Q(T)$. The higher-order terms are functions of the frequencies raised to successively higher negative exponents and, hence, should have a negligible effect as higher modes are used providing the time-function term does not grow proportionally.

The effect of damping on the accuracy of the response is shown in figures 6a and 6b. Increasing the modal damping ζ_i does not always increase the accuracy of the MAM as suggested in reference 11. For the case of a uniformly loaded cantilevered beam subjected to a step loading, studied in reference 11, the accuracy of the MAM is enhanced in the presence of damping as can be seen from eq. (33). Since all the derivatives of the forcing function vanish, the only terms remaining are the pseudo-static response and a term which is a function of $e^{-\zeta_r \omega_r t}$. Hence, as ζ_i increases, the relative importance of this term on the solution, as compared to the pseudo-static response term ($K^{-1} Q(T)$), decreases and, therefore, the

accuracy of the MAM increases. For other forcing functions, there are additional terms which increase in importance as damping increases (see, for example, eq. (38) and ref. 13) and so the effect of ζ_i on accuracy is more complex. For example, for the case of a linearly time-varying forcing function, the last term in eq. (38) decreases exponentially as the damping increases (see eq. (33)); however, the second term increases proportionally as ζ_i increases (the third term vanishes since $\ddot{Q}(T) = 0$). If the magnitude of the second term (eq. (38)) does not decrease with respect to the first term, an increase in damping will not necessarily result in an increase in accuracy as it does in the unit step function case. Notice that the FDM and DCM are much more accurate than either the MDM or MAM for the range of time and damping levels considered.

4.1.1.2 Step Load.- The step forcing function is discontinuous at time T = 0 and hence the integration-by-parts of the convolution integral is assumed to begin at time $T = 0^+$. Including the discontinuity in the integration-by-parts results in jump conditions which must be included at times during which there are discontinuities in the forcing function and its time derivatives (ref. 38). The MAM, FDM, and DCM produce the same results for a step forcing function because for T > 0, Q(T) is constant and all its derivatives vanish (see, for example eq. (38)). As shown in figure 7, the MAM, FDM, or DCM are more accurate than the MDM. A plot of moment error, using the first 25 modes, as a function of time is shown in figure 8. Over the time range considered (T = 0.001-0.01) the moment errors of the higher-order methods are about one-half the magnitude of the error using the MDM at time T = 0.001. Also, as time increases, the error associated

with each method for a given number of modes used tends to decrease and at time T = 0.01, the error using the higher-order methods is an order of magnitude lower than the MDM.

For a discontinuous forcing function, such as a unit step, $\mu(T)$ at T = 0, the MDM exactly predicts a zero response at time T = 0. The higher-order methods ($N \geq 1$), however, require a summation of all the modes to exactly predict a zero response or the inclusion of appropriate jump conditions. Therefore, the MDM will produce qualitatively better results for times near T = 0 or close to discontinuities. To calculate the transient response accurately at very small times, a large number of modes is necessary. The displacement distribution for a unit step loading at time T = 0.0002 and ζ_i = 0.05 which was calculated using 25 modes is shown in figure 9. As expected, the MAM, FDM, and DCM results are equivalent and more accurate than results obtained using the MDM. The moment error norm associated with the higher-order methods is exceedingly large, at time T = 0.0002, when fewer than five modes are used to approximate the response (Fig. 10). If a sufficient number of modes is used to predict the displacement distribution accurately (m > 24), the higher-order methods appear to give better results.

Hence, for discontinuities in the forcing function and its time derivatives, the higher-order modal methods should include the appropriate jump conditions. The jump conditions are necessary because the integration-by-parts of the convolution integral requires that the functions and their derivatives are continuous. If the jump conditions are not accounted for in the higher-order modal methods, there will be

solution errors close to the time of the discontinuity as seen in the previous problem.

4.1.2 *Multispan Beam*

The second problem studied is a simply-supported, uniform multispan beam (10 equal-length spans) subject to two loading distributions and one forcing function. A nominal frequency, $\omega_0 = \sqrt{\frac{EI}{\rho AL^4}}$ rad/sec, is used to normalize time, t, such that $T = \omega_0 t$. The first 30 normalized natural frequencies of the beam are listed in Table 2. An analytical solution for the mode shapes and frequencies of multispan beams was obtained using equations from reference 41. This problem was selected because the frequencies are closely spaced (in groups equal to the number of spans, 10 in this example) and the chances of a neglected higher mode having a considerable effect on the response is increased.

4.1.2.1 Uniform Quintic Time-Varying Load.- For this case the load distribution is uniform and varys in time as $Q(T) = 1000(T^4 - T^5)$, where T is the normalized time. The moment distribution, normalized by the maximum value of the moment M of the multispan beam at $T = 1.2$ and $\zeta_i = 0.05$ is shown in figure 11. The FDM and DCM are accurate even when only one mode is used, whereas the MDM and MAM require 30 and 10 modes, respectively, for acceptable accuracy ($e < 0.01$). The spatial moment error norm, e, as a function of the number of modes for $T = 1.2$ is

shown in figure 12. The first nine modes are nearly orthogonal to the uniform load distribution, hence the modal load $\phi_r^T Q(T)$ is negligible and has a negligible effect on the MDM response (see fig. 12). The 10th and 30th modes, however, have an effect on the solution as shown in figure 12. The effect of these higher modes, however, is taken into account to some degree by the pseudo-static response (note the MAM curve for $m < 10$) and to a greater degree by the higher-order approximation of the neglected modes used in the FDM and DCM methods. Hence, the FDM and DCM using only one mode calculate a more accurate moment response than the MDM using 49 modes or the MAM using nine modes. The spatial moment error norm is shown in figure 13 as a function of time for each method (using 10 modes). The accuracy of the FDM is at least two orders of magnitude greater than the MDM and at least one order of magnitude greater than the MAM. The DCM was, in general, more accurate than the FDM. The MDM and MAM are equivalent at $T = 1.0$, as expected, because $Q(T) = 0$. At $T = 1.0$ the error associated with the MDM decreases an order of magnitude and that associated with the MAM increases an order of magnitude as shown.

4.1.2.2 Discrete Quintic Time-Varying Load.- For this loading distribution, the solution does not converge in a step-like manner as in figure 12 but does so gradually and at a slower rate as shown in figure 14. This convergence occurs because the loading distribution is not nearly orthogonal to many mode shapes and hence the associated modal load, $\phi_r^T Q(T)$, is not negligible as it was for the uniform distribution. Once again,

the FDM and DCM converge more rapidly than either of the other, lower-order modal methods. The DCM converges faster than the FDM for $T > 0.2$. The DCM and FDM both experience similar error at times $T = 0.2$ shown in figure 15. As time progresses, the DCM appears to be more accurate than the FDM. Once again, the accuracy or these higher-order modal methods (FDM and DCM) are several orders of magnitude greater than the lower-order methods (MDM and MAM). In addition, the accuracy of the higher-order methods tends to increase as T increases (see fig. 15).

4.2 Non-Proportional Damping

4.2.1 Two Degree-of-Freedom Spring-Mass-Damper System.- A simple, two-degree-of-freedom spring-mass-damper problem (see fig. 16) with a sinusoidal forcing function was analyzed to compare the accuracy of the MDM, MAM, FDM, and DCM. For this problem $M_1 = M_2 = 1$ Kg, spring constants $K_1 = K_2 = 1000$ N/mm, and damping constant C = 1 N-s/mm. This problem was also investigated in reference 39 and included in that reference are the particular solutions for polynomial as well as sinusoidal forcing functions. The sinusoidal forcing function, $\sin(\omega_f t)$, is applied to the second mass as shown in figure 16. The natural frequencies are $\omega_1 =$ 19.54 rad/s and $\omega_2 =$ 51.17 rad/s. The system is proportionally damped (Λ is diagonal in eq. (38)) if $\alpha = K_1/K_2$ (ref. 42). Hence, proportional damping occurs for a value of $\alpha = 1.0$. The accuracy of each method is assessed by a time-integrated error norm (eq. 46) where $u_i(t)$ is the calculated response using all the modes and $u_i^a(t)$ is the approximate response using a subset of the modes. Results were calculated using both the real and damped modes (eqs. (26) and (39), respectively). The modal coordinates, q and Z, were calculated by numerically integrating equations (7) and (30), respectively, using a Runge-Kutta method. For this problem, the FDM used was of order four (N = 4 in eqs. (26) and (39)). The time, τ, selected for integrating the error was chosen to be $\tau = 16\pi/\omega_f$.

Results of the error as a function of the forcing frequency using one real mode for the proportionally-damped case (α =1.0) is shown in figure 17. In general, the forcing function frequency must be lower than the highest natural frequency used in the approximate modal response for accurate results. As shown in figure 17, the accuracy increases as the order of the modal method increases. The results for the lower range of frequencies are shown more clearly in figure 18, which is an expanded error scale of figure 17. The results for the FDM (N=4) and DCM are similar and more accurate than the lower order methods such as the MDM (N=0) and the MAM (N=1) for ω_f < 20 rad/s. For ω_f > 20 rad/s, the DCM remains slightly more accurate than the FDM; however, as the forcing frequency approaches the second natural frequency (ω_f= 51.17 rad/s), all methods produce inaccurate results. Results using one real mode or two damped modes are identical for the proportionally-damped case.

Results for the non-proportionally-damped case (α = 20) using two damped modes are shown in figure 19. Results are similar to the proportionally-damped case with the exception that the DCM exhibits surprisingly good results at forcing function frequencies close to the second natural frequency. This result is unexplained at present and is believed to be fortuitous and, hence, it is recommended that all modal methods should include modes whose frequencies exceed the frequency of the forcing function. A comparison of the damped-mode solution (using two damped modes (eq. (26)) and the undamped solution (using one real mode (eq. (39)) is shown in figure 20 for the non-proportionally-damped case (α = 20). As shown in figure 20, the damped-mode solution using two damped modes (dashed lines) produces more accurate results than those using only

one real mode (solid lines). The damped-mode solution for the FDM and DCM are nearly equivalent and result in the smallest error for frequencies as large as 30 rad/s. Hence, it may be beneficial, in some cases, to use the damped modes to obtain a more accurate solution.

The FDM produced results that are similar to the DCM results for forcing frequencies below the first natural frequency. A comparison of the modal methods for a forcing frequency $\omega_f = 10$ rad/s is shown in figure 21. Once again, the higher-order modal methods result in more accurate solutions. The large relative errors near $\tau = 0$ are due to the zero initial conditions which cause the denominator of eq. (46) to approach zero at $\tau = 0$. As explained in reference 13, the increase in accuracy with the order of the modal method is due to the addition of terms which are functions of the generalized stiffness and mass matrices and the force vector and its time derivatives. These additional terms approximate the effect of the higher modes which were neglected in the modal summation.

4.2.2 Multispan Beam with Discrete or Uniform Damping and Uniform Loading - A multispan beam (five spans) with discrete or uniform damping and uniform loading, is shown in figure 22. A similar problem was also studied in references 22 and 23. This problem was chosen because it not only includes the effect of nonproportional damping, but also the effect of discrete damping. The load history was changed in the present study, to a uniform quintic varying load. The modulus of elasticity $E = 10 \times 10^5$ lbs/in.^{2}, density $\rho = .28$ lbs/in.^{3}, and damping constants are $C_1 = 0.008$ lbs-sec/in and $C_2 = 1.2$ lbs-sec/in. The finite element method was used to

discretize the problem in space. Three conventional beam elements (ref. 23) per span were used to represent the five-span beam as shown in figure 22. Results of moment error for the case of discrete damping at time t = 1.2 sec are shown in figure 23. Similar to previous results, the higher-order methods are consistently more accurate; the FDM and DCM have errors e < 0.01 using only one mode, whereas the MAM and MDM require 5 and 15 modes, respectively, for comparable accuracies. The DCM is shown to be an order of magnitude more accurate than the FDM at time T = 1.2. Similar results for a proportionally damped case where $\zeta_i = 0.05$ are shown in figure 24. For the case of proportional damping, the DCM and FDM results are very similar; for the case of discrete damping (fig. 23), the DCM results are almost an order-of-magnitude better than the FDM.

Table 1. Natural frequencies of a cantilevered beam $\left(\omega_0 = \sqrt{\frac{EI}{\rho AL^4}} \text{ rad/sec} \right)$.

MODE NUMBER	NORMALIZED NATURAL FREQ. ω / ω_0
1	3.52
2	22.03
3	61.70
4	120.90
5	199.86
6	298.56
7	416.99
8	555.17
9	713.17
10	890.73
11	1088.12
12	1305.26
13	1542.13
14	1798.74
15	2075.08
16	2371.17
17	2687.00
18	3022.57
19	3377.87
20	3752.92
21	4147.70
22	4562.22
23	4996.49
24	5450.49
25	5924.23
26	6417.71
27	6930.93
28	7463.89
29	8016.59
30	8589.02

Table 2. Natural frequencies of a simply-supported multispan beam (10 spans) $\left(\omega_0 = \sqrt{\frac{EI}{\rho AL^4}} \text{ rad/sec}\right)$.

MODE NUMBER	NORMALIZED NATURAL FREQ. ω / ω_0
1	9.87
2	10.15
3	10.94
4	12.17
5	13.70
6	15.42
7	17.25
8	19.07
9	20.75
10	21.91
11	39.48
12	40.07
13	41.72
14	44.11
15	46.90
16	49.96
17	53.12
18	56.23
19	58.95
20	60.95
21	88.83
22	89.78
23	92.23
24	95.74
25	99.87
26	104.25
27	108.88
28	113.29
29	117.13
30	119.97

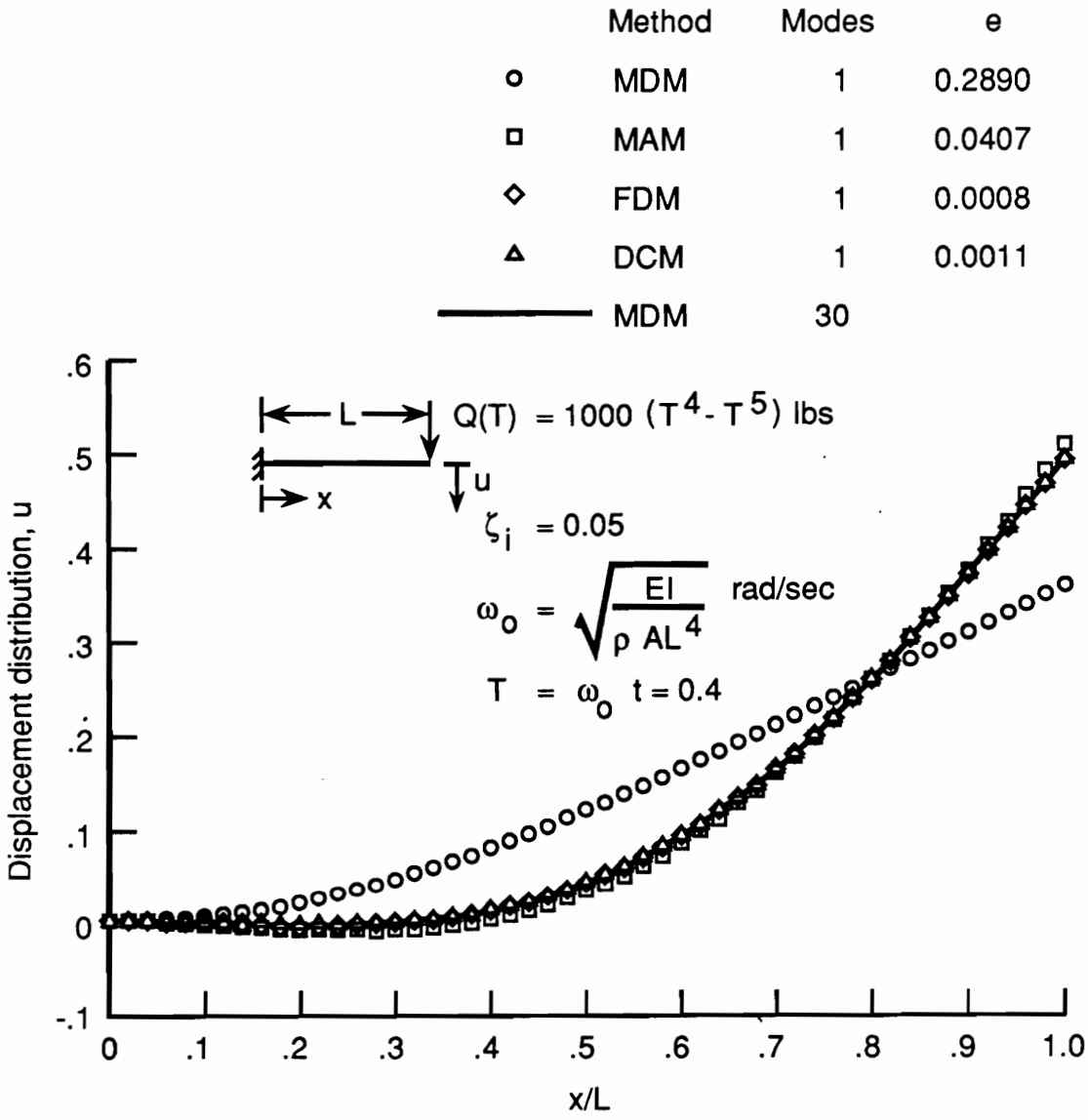

a) Displacement distribution

Figure 1. Representation of displacement and moment errors in a cantilevered beam with tip loading using spatial error norm e (Q(T) = 1000(T^4 - T^5) lbs., T = 0.4, and damping ratios ζ_i = 0.05).

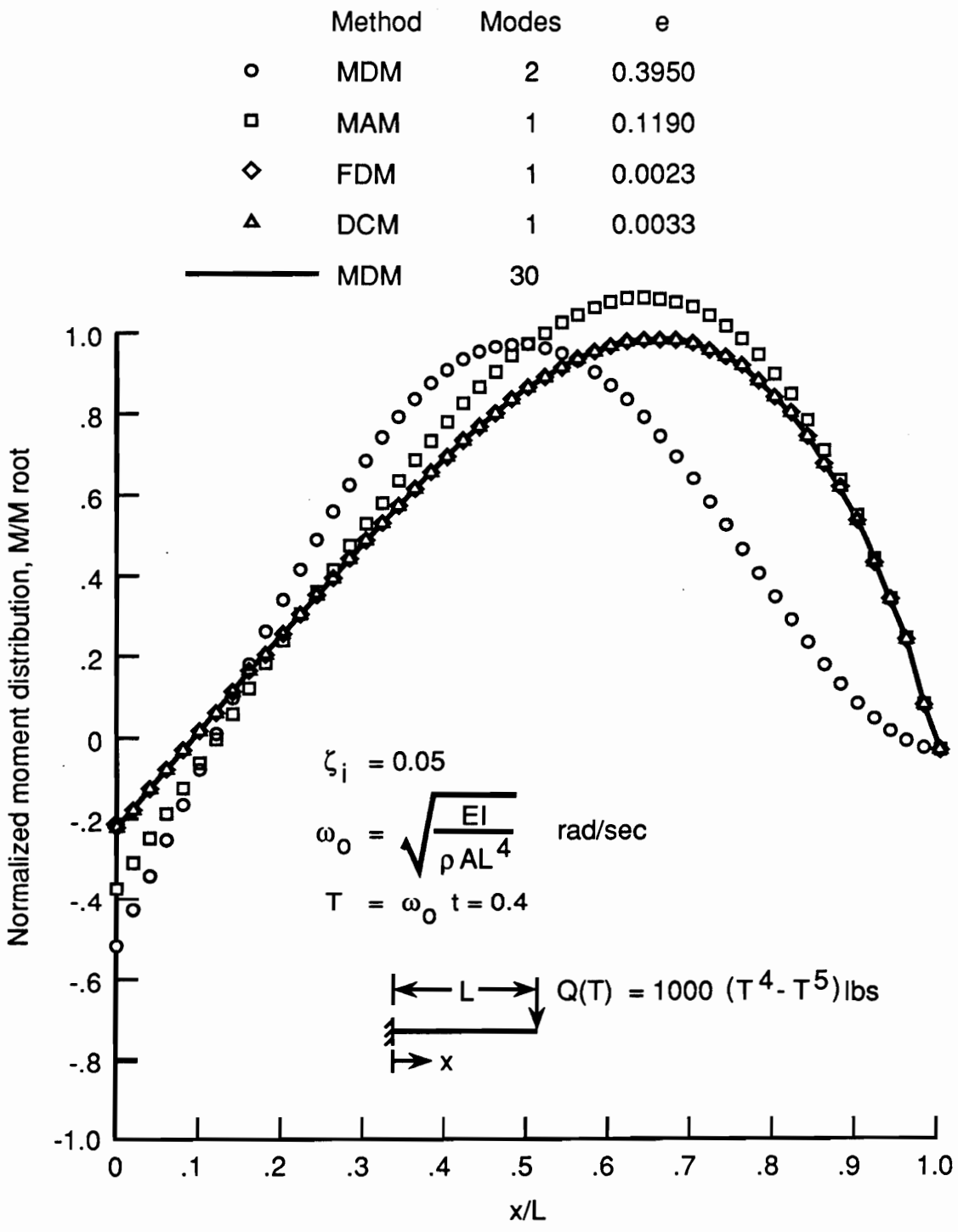

b) Moment distribution

Figure 1. Concluded.

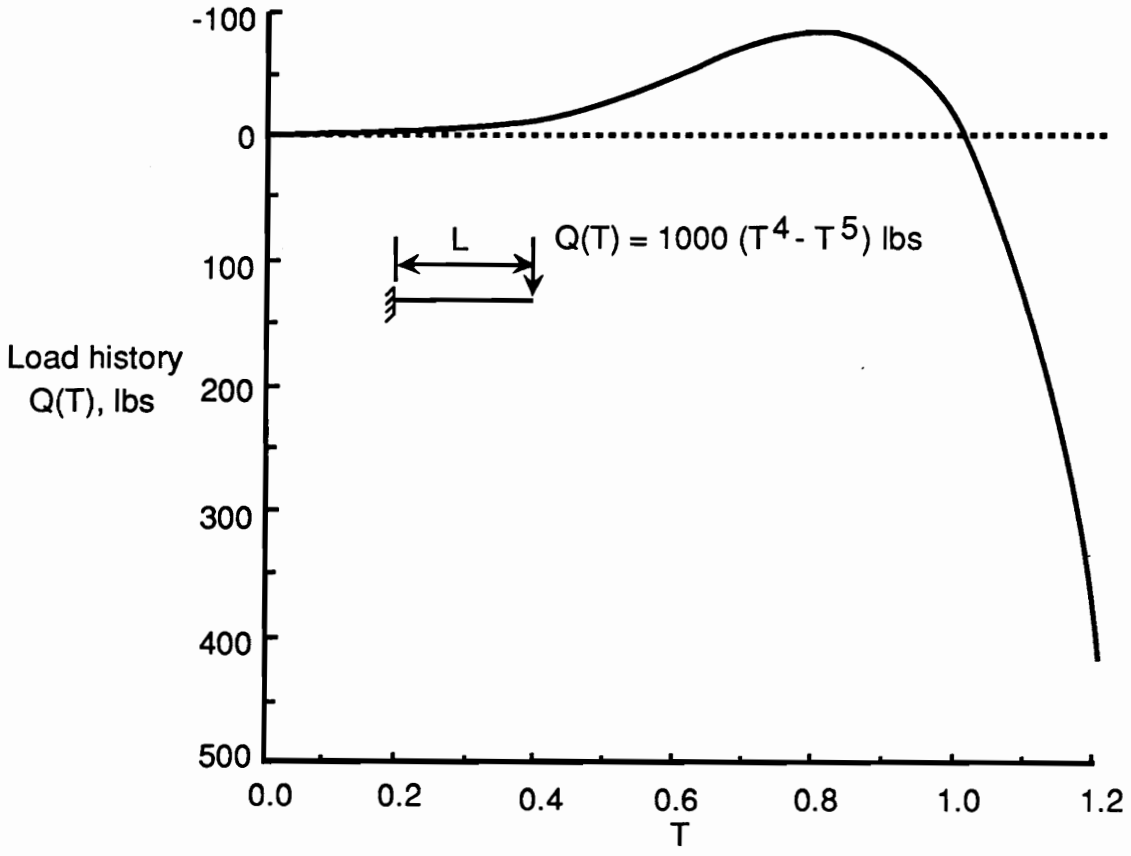

a) Force history

Figure 2. Cantilevered beam with zero damping ($\zeta_i = 0.0$) subject to a tip load $Q(T) = 1000(T^4 - T^5)$ lbs.

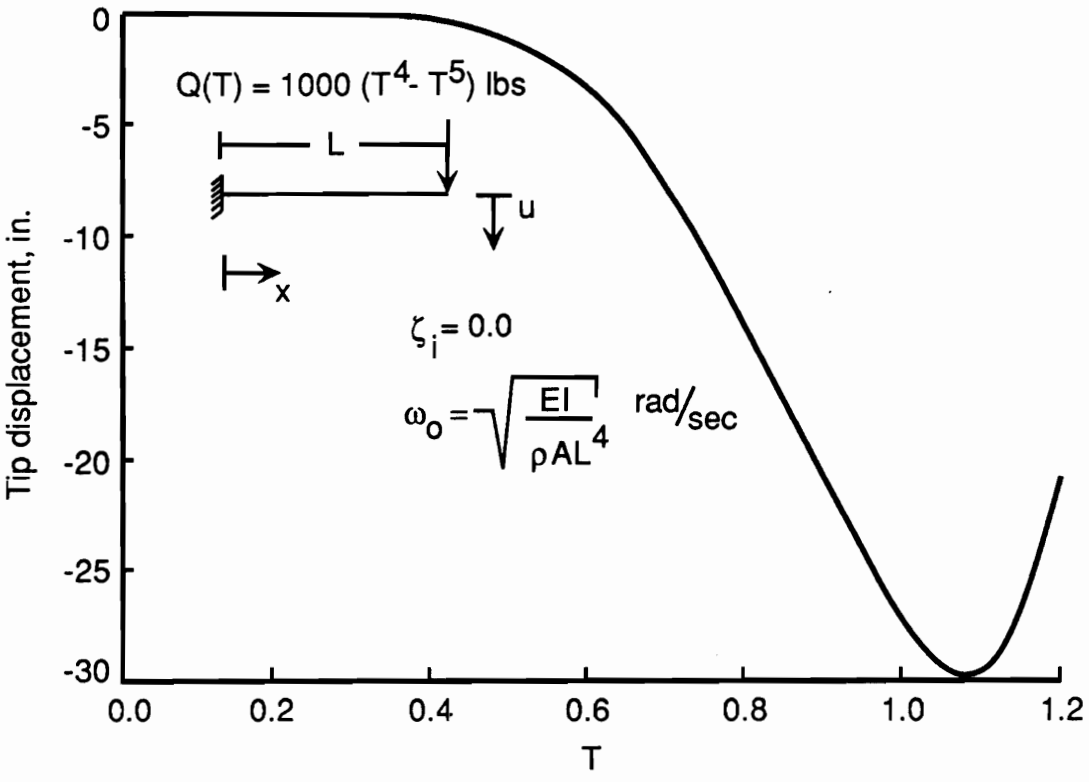

b) Tip displacement

Figure 2. Concluded.

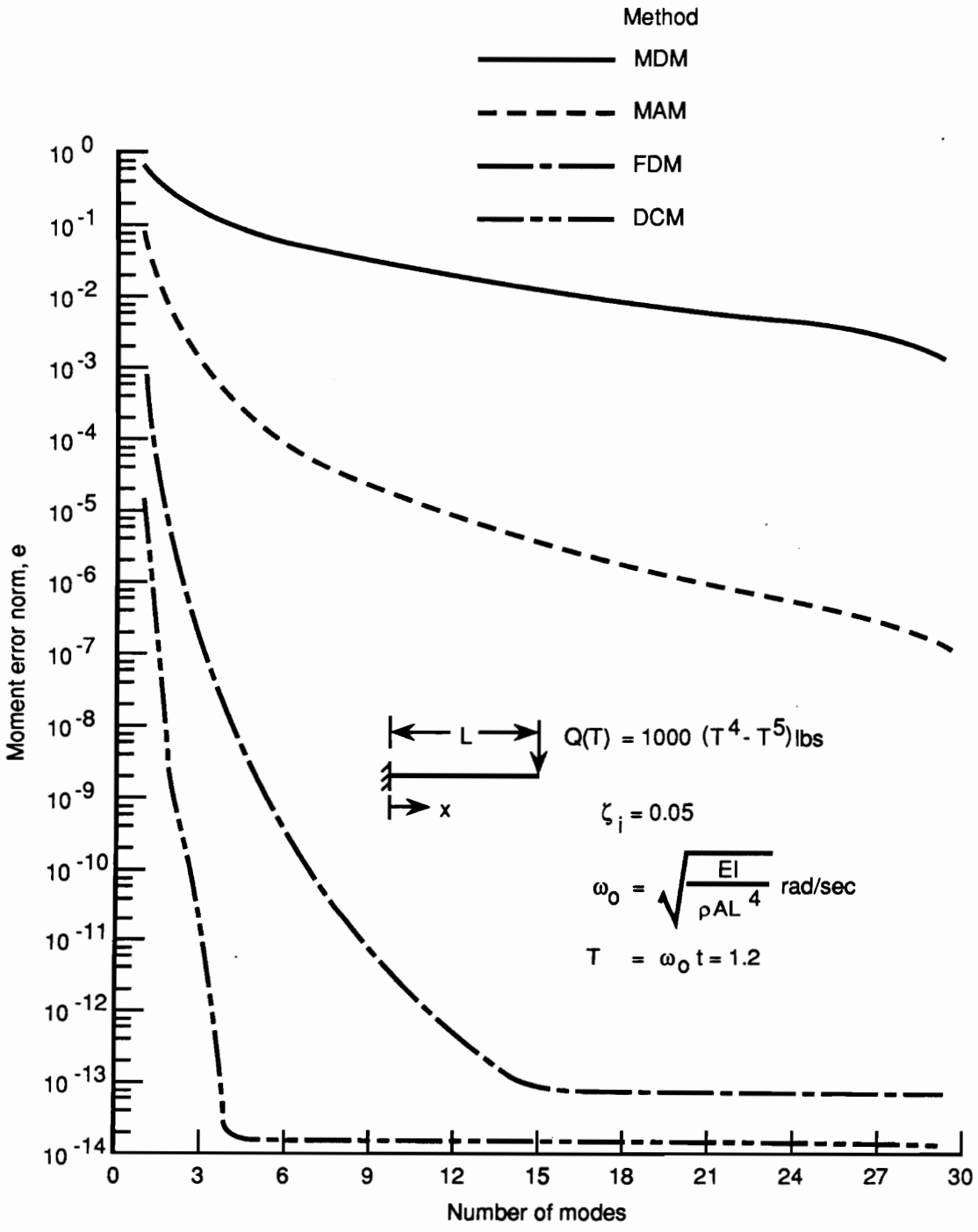

Figure 3. Comparison of moment errors of a cantilevered beam subject to a tip load $Q(T) = 1000(T^4 - T^5)$ lbs., where $T = 1.2$ and damping ratios $\zeta_i = 0.05$ for four different modal methods.

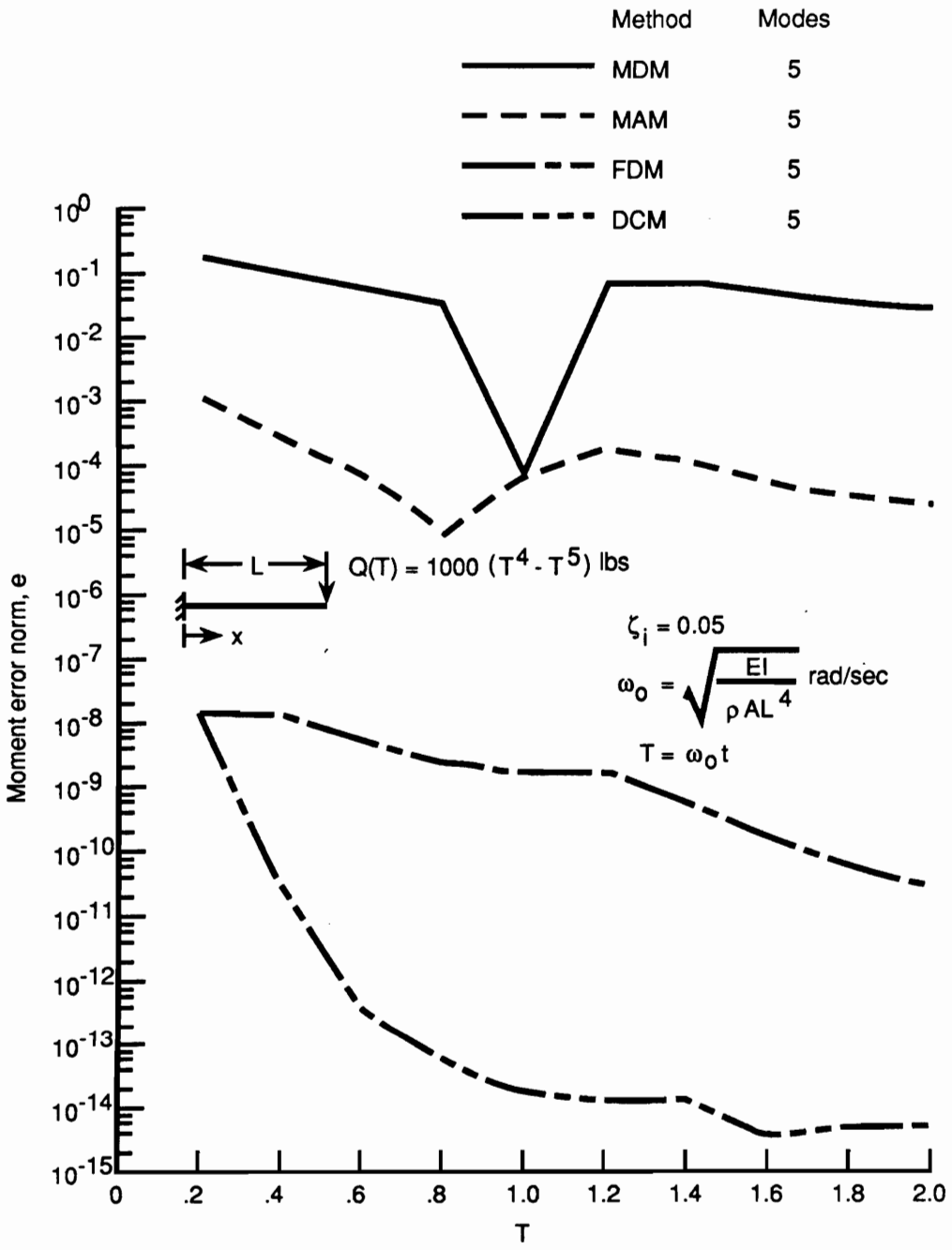

Figure 4. Variation of moment errors as a function of time, using 5 modes in the modal summation. Cantilevered beam with a tip load $Q(T) = 1000(T^4 - T^5)$ lbs. and where damping ratios $\zeta_i = 0.05$.

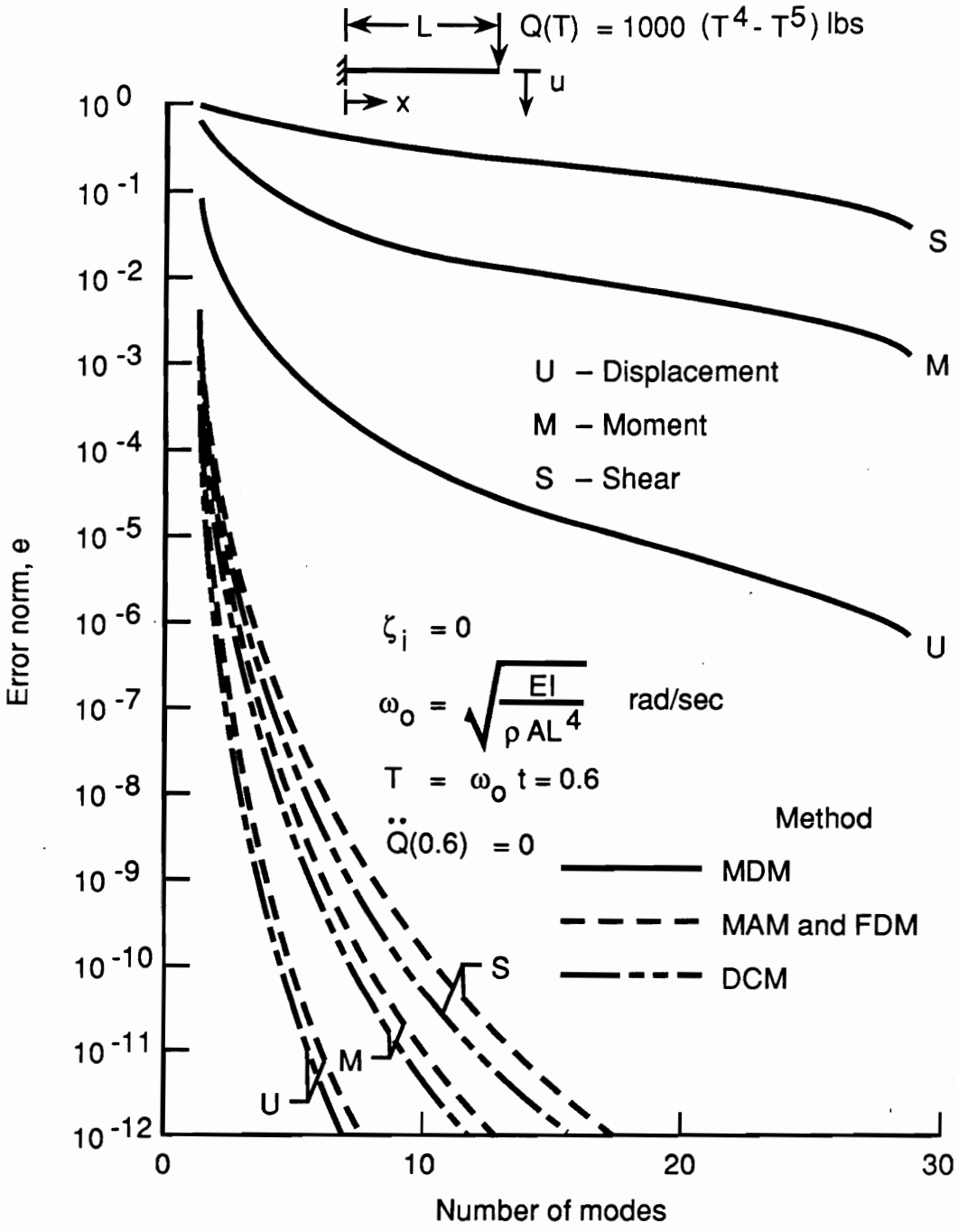

a) T = 0.6

Figure 5. Comparison of displacement, moment, and shear errors of a cantilevered beam using four different modal methods (tip load $Q(T) = 1000(T^4 - T^5)$ lbs. and damping ratios $\zeta_i = 0.0$).

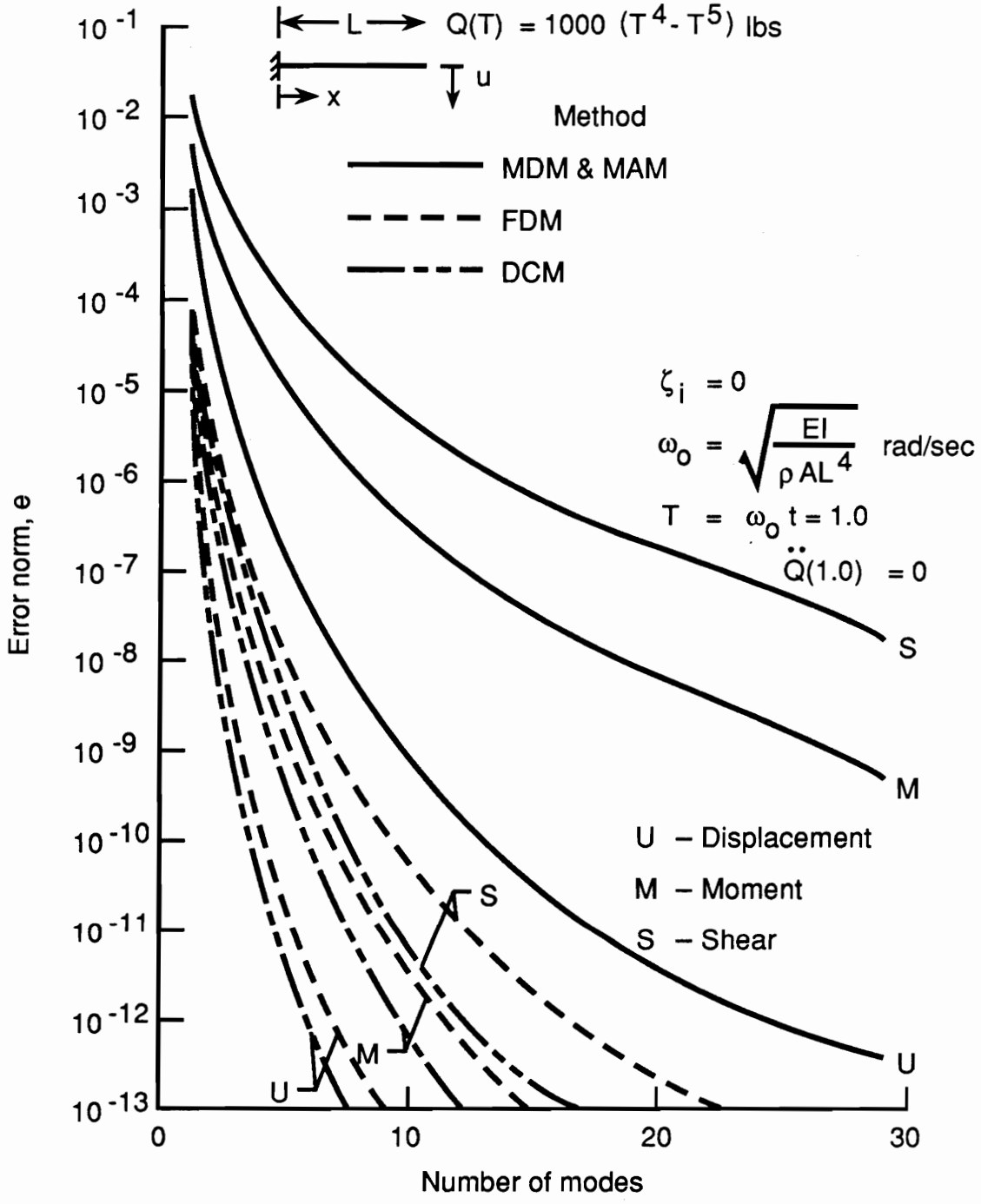

b) T = 1.0

Figure 5. Concluded.

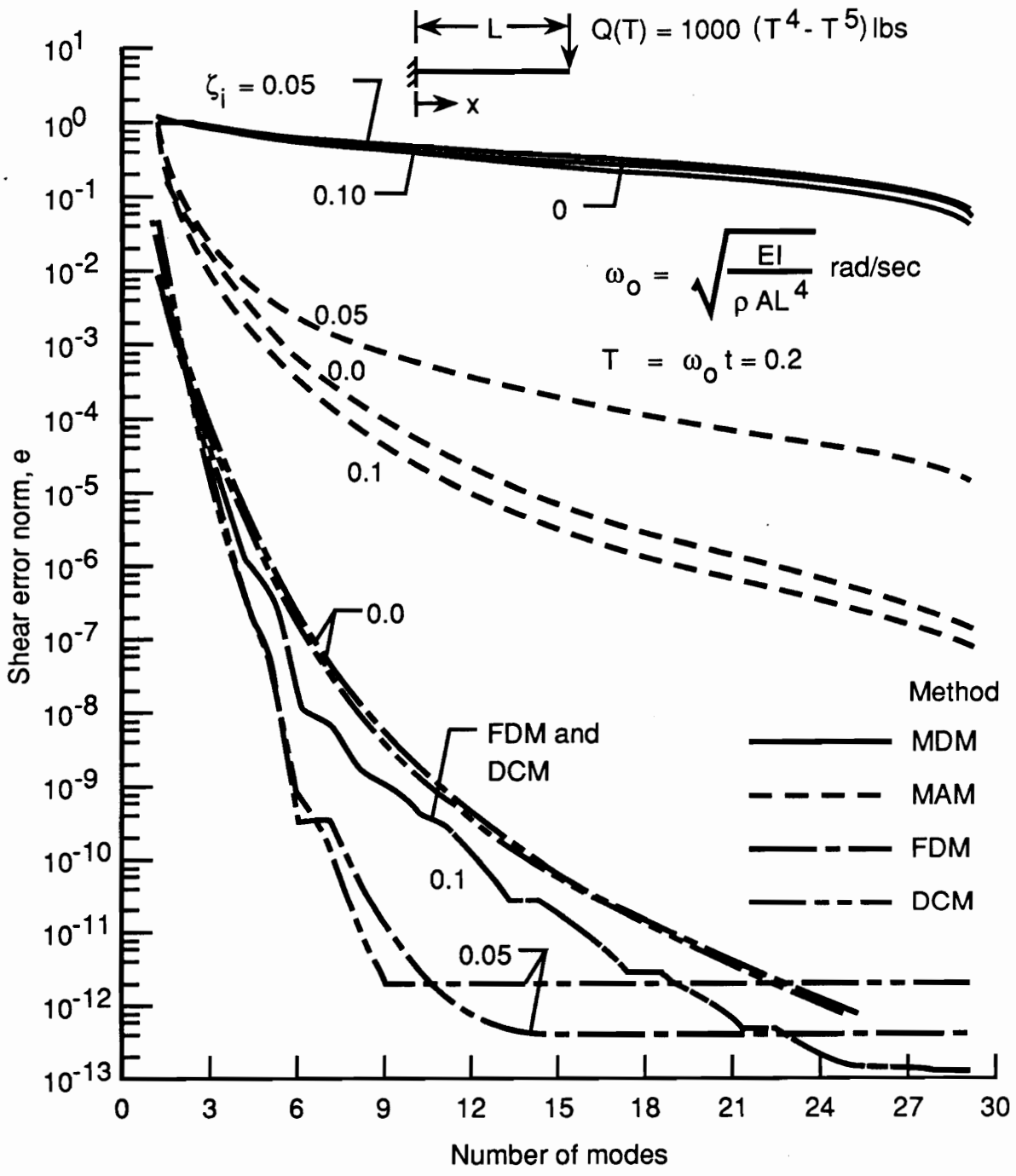

a) T = 0.2

Figure 6. Comparison of shear errors of a cantilevered beam for various damping levels (tip load $Q(T) = 1000(T^4 - T^5)$ lbs.).

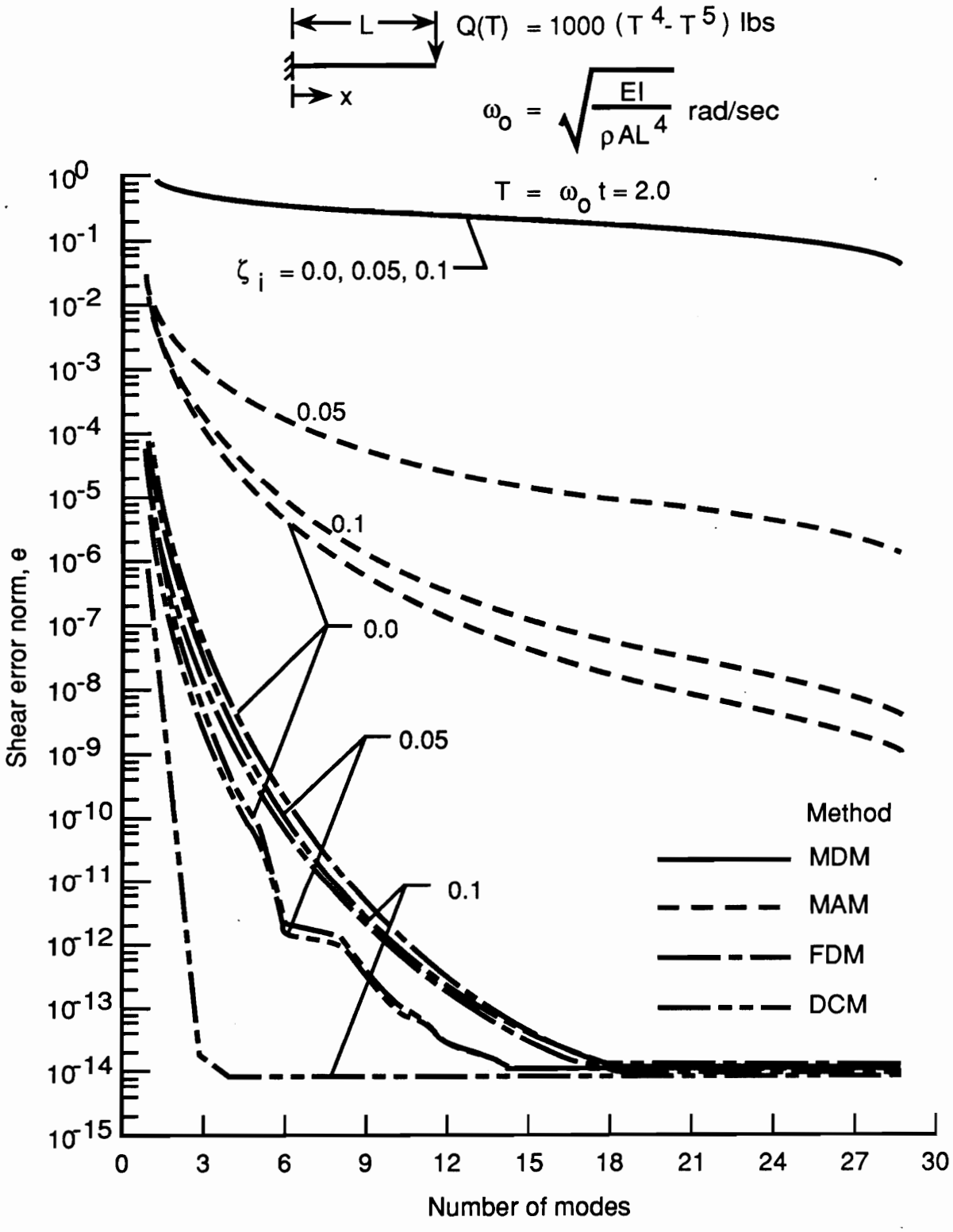

b) T = 2.0

Figure 6. Concluded.

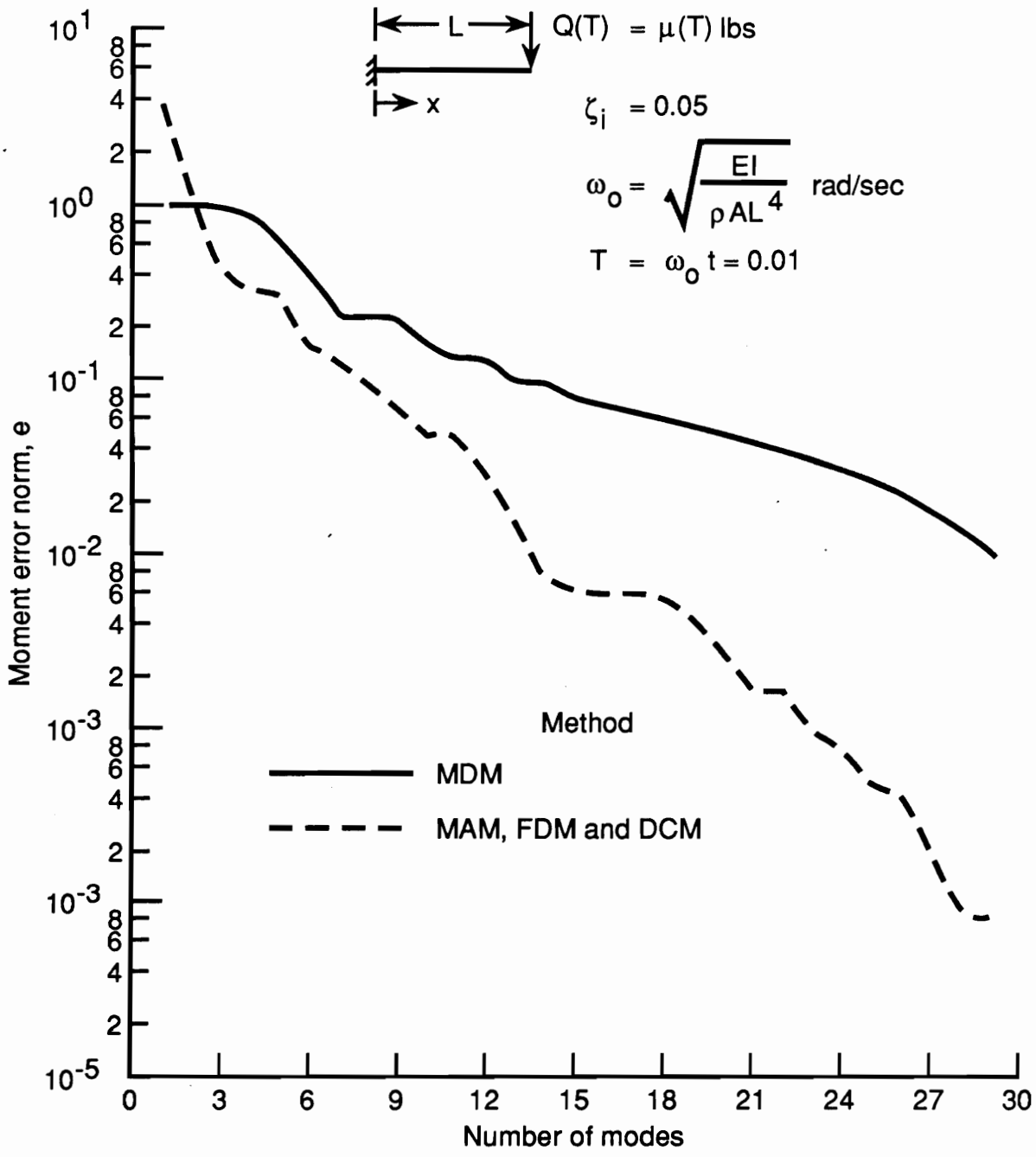

Figure 7. Comparison of moment errors of cantilevered beam subject to a unit step tip loading Q(T) = μ(T) lb., where T = 0.01 and damping ratios ζ_i = 0.05 for four different modal methods.

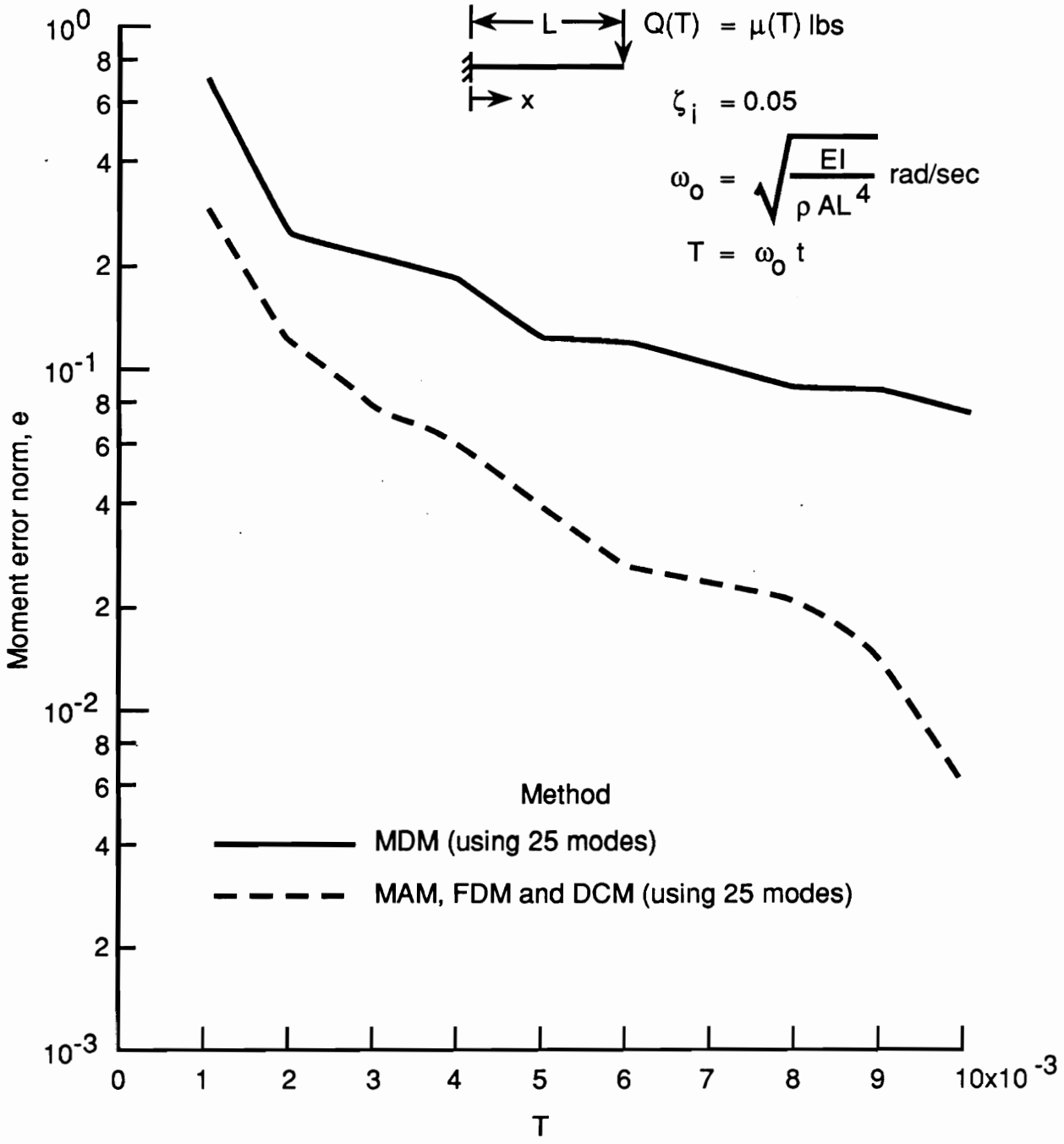

Figure 8. Variation of moment errors as a function of time, assuming 25 modes are used in the modal summation, for a cantilevered beam with a unit step tip loading ($Q(T) = \mu(T)$ lb. and damping ratios $\zeta_i = 0.05$).

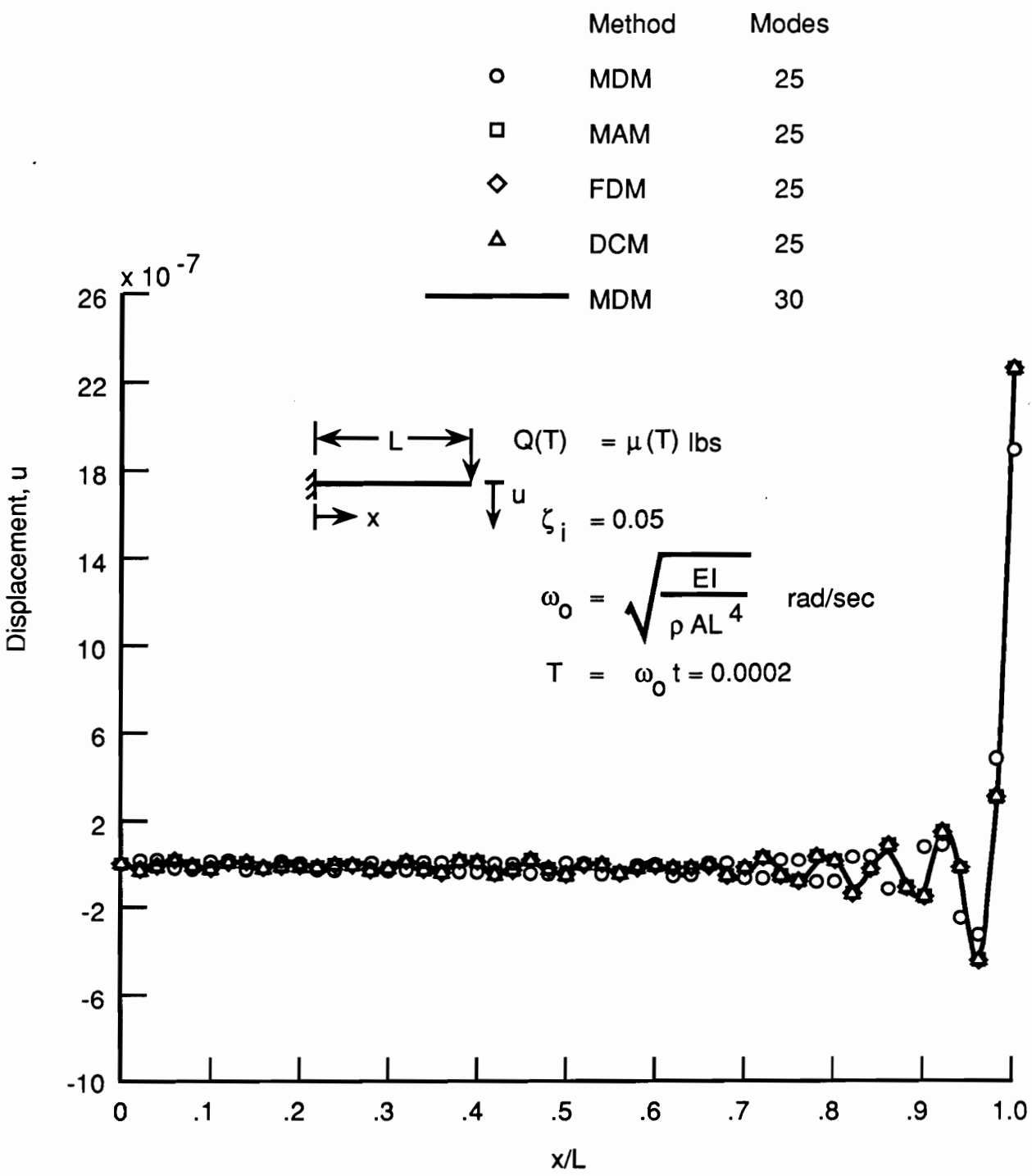

Figure 9. Displacement distribution in a uniform cantilevered beam with a unit step tip loading at time T = 0.0002 (Q(T) = μ(T) lb. and damping ratios ζ_i = 0.05).

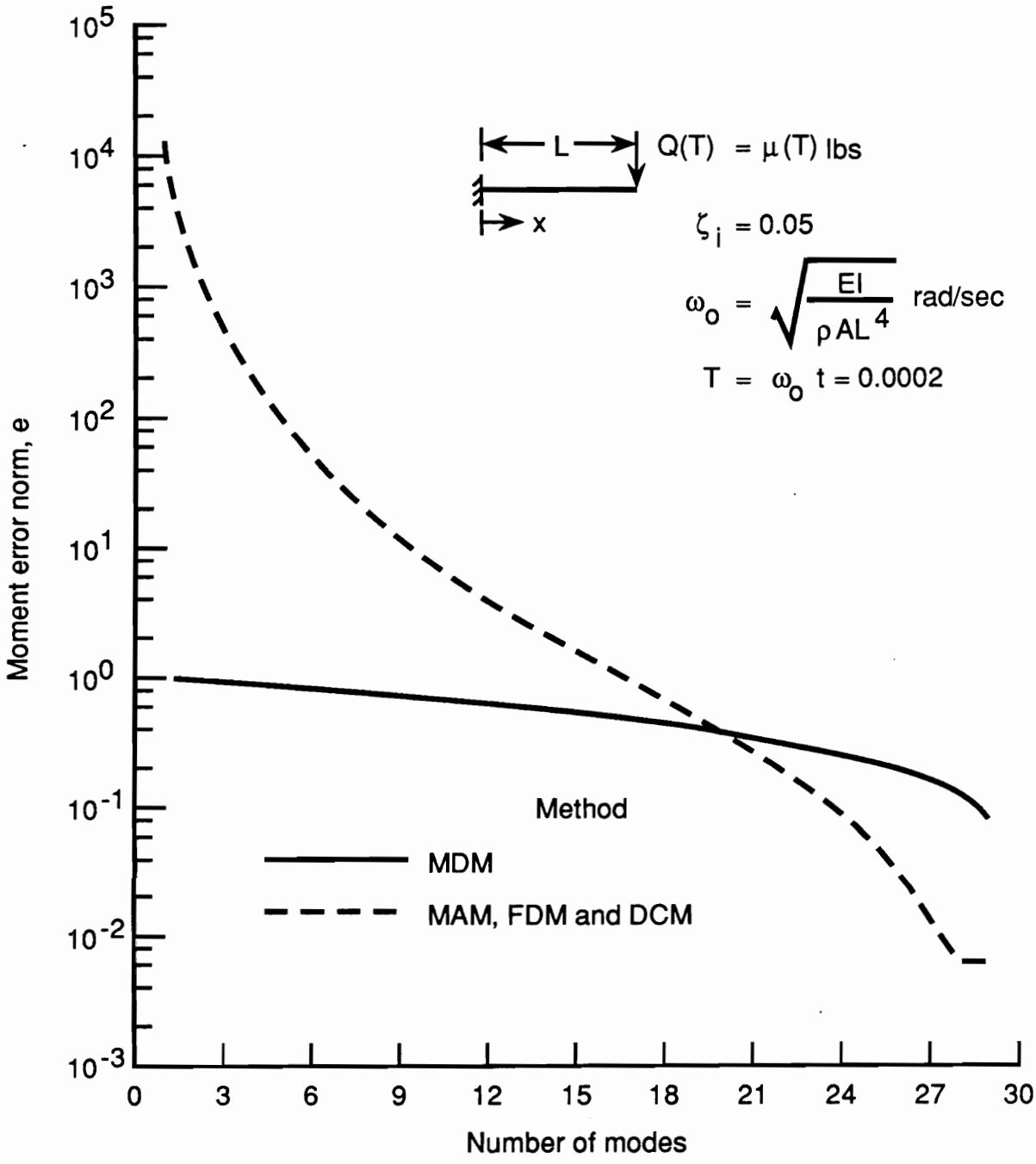

Figure 10. Comparison of displacement errors for a uniform cantilevered beam subject to a unit step tip loading at time T = 0.0002 (Q(T) = μ(T) lb. and damping ratios ζ_i = 0.05).

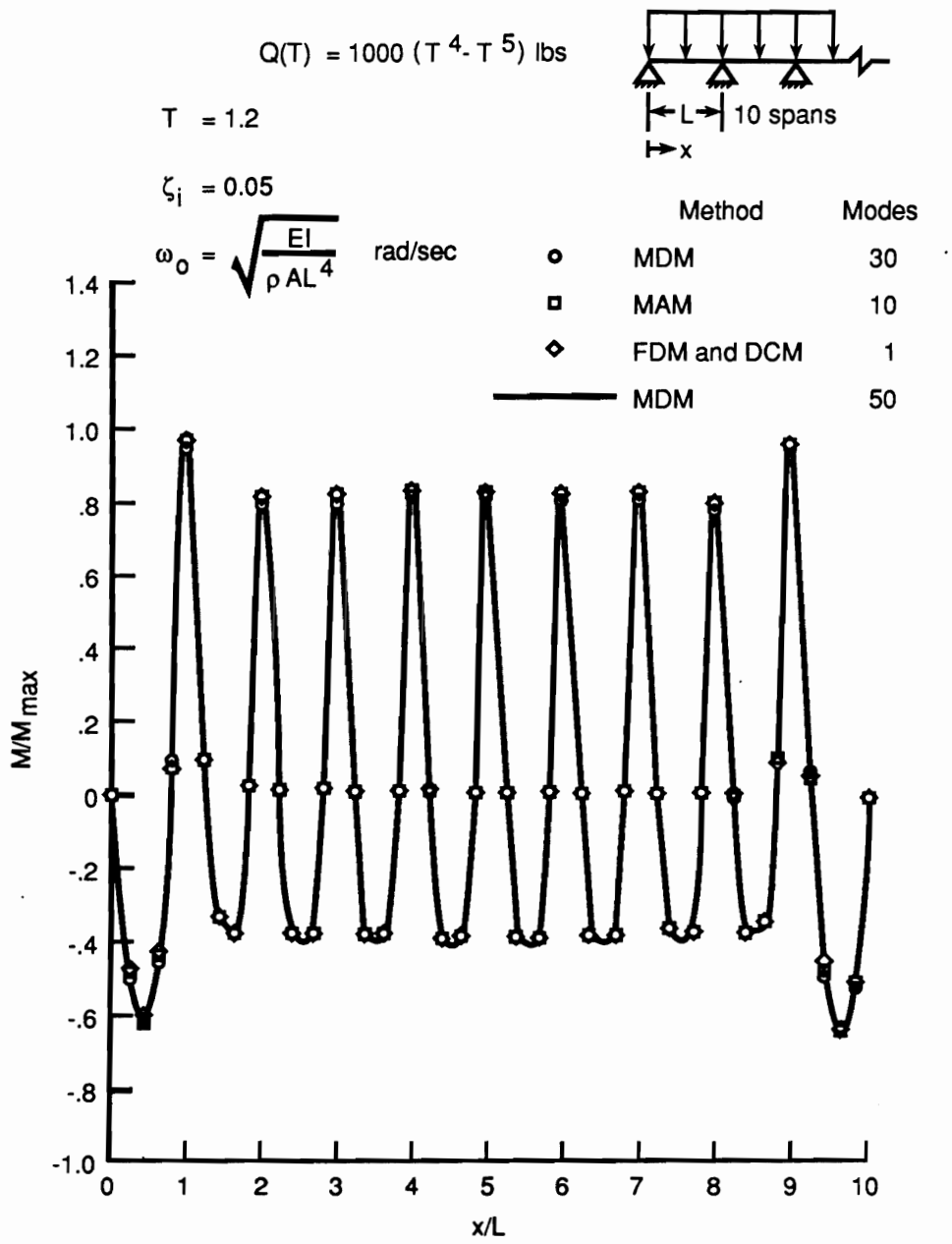

Figure 11. Comparison of normalized moment distributions along a simply-supported multispan beam (ten equally-spaced spans) and a uniformly-distributed load varying with time as $Q(T) = 1000(T^4 - T^5)$ lbs./in., where $T = 1.2$ and damping ratios $\zeta_i = 0.05$.

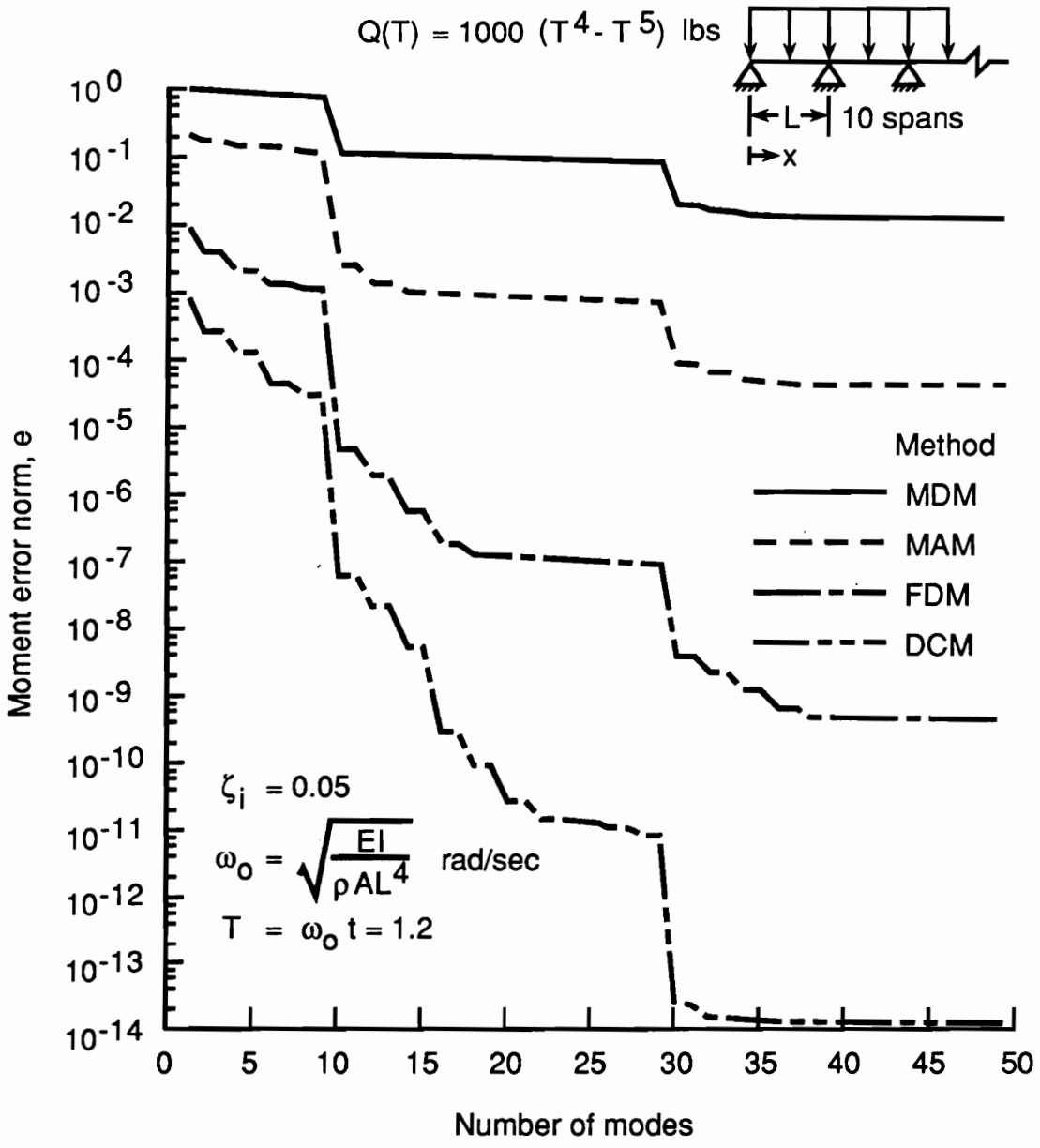

Figure 12. Comparison of moment errors of a simply-supported multispan beam (ten equally-spaced spans) subject to a uniformly-distributed load varying with time as $Q(T) = 1000(T^4 - T^5)$ lbs./in., where $T = 1.2$ and damping ratios $\zeta_i = 0.05$.

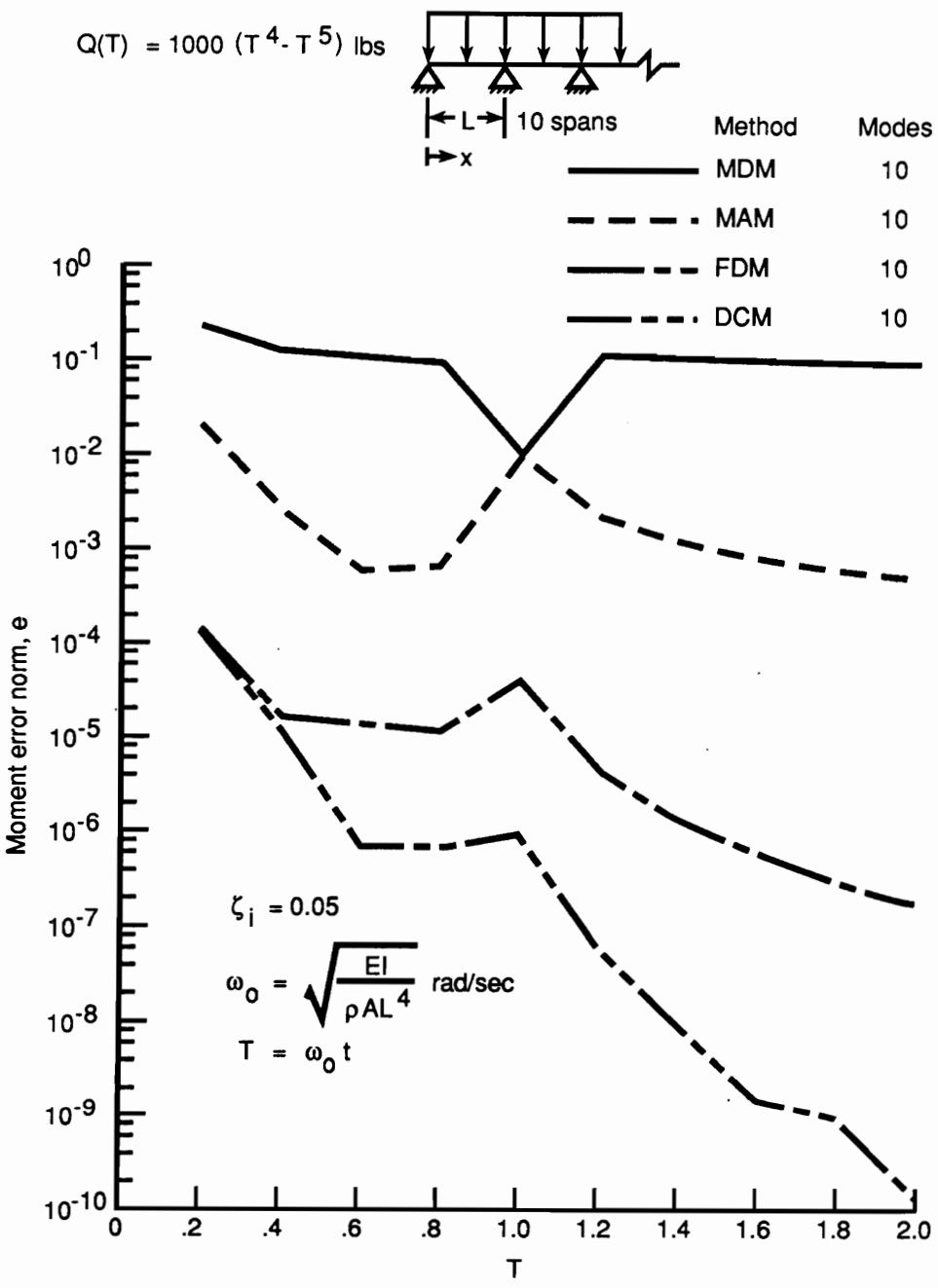

Figure 13. Variations of moment errors as a function of time, using ten modes in the modal summation, for a simply-supported multispan beam (ten equally-spaced spans) subject to a uniformly-distributed load varying with time as $Q(T) = 1000(T^4 - T^5)$ lbs./in. (where damping ratios $\zeta_i = 0.05$).

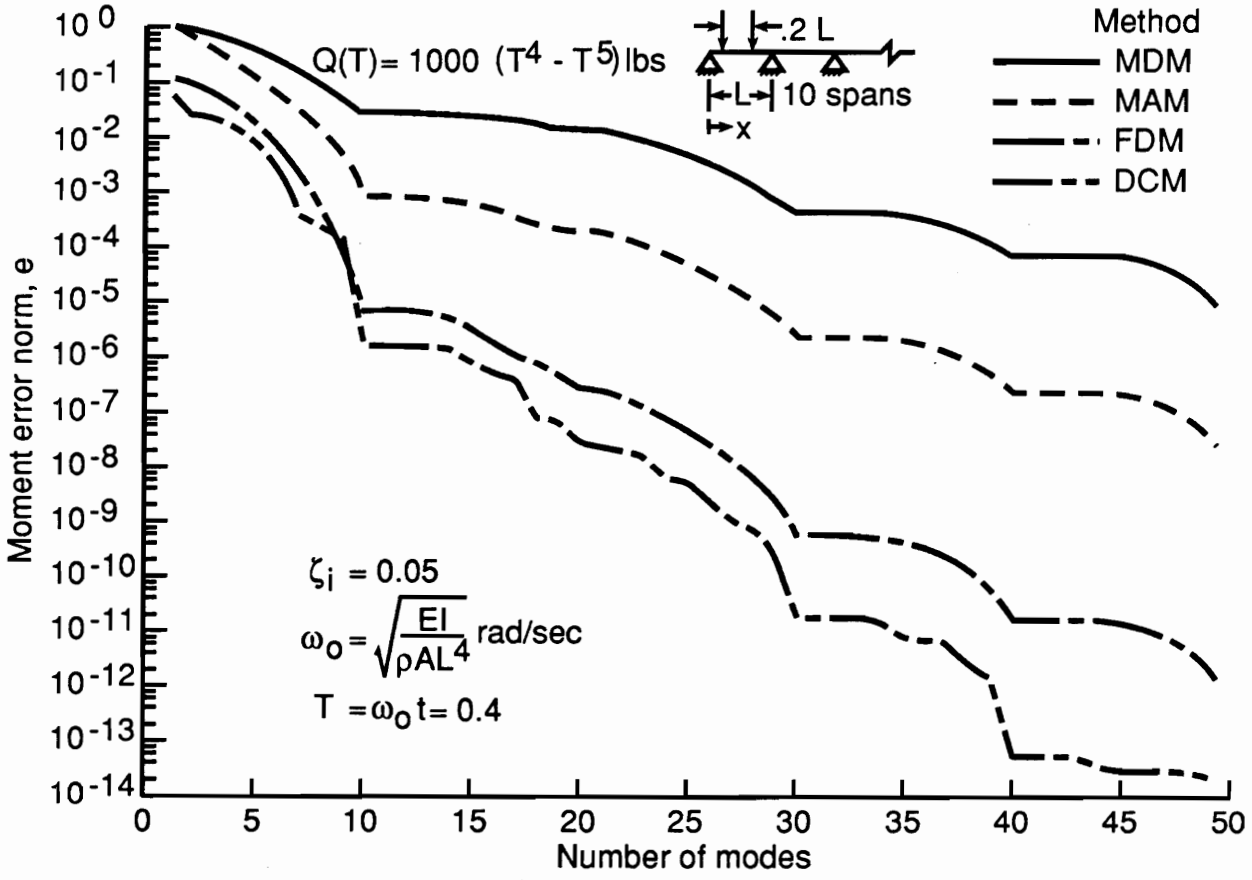

Figure 14. Comparison of moment errors of a simply-supported multispan beam (ten equally-spaced spans) subject to two concentrated loads spaced about the center of the first span and varying in time as $Q(T) = 1000(T^4 - T^5)$ lbs., where $T = 0.4$ and damping ratios $\zeta_i = 0.05$.

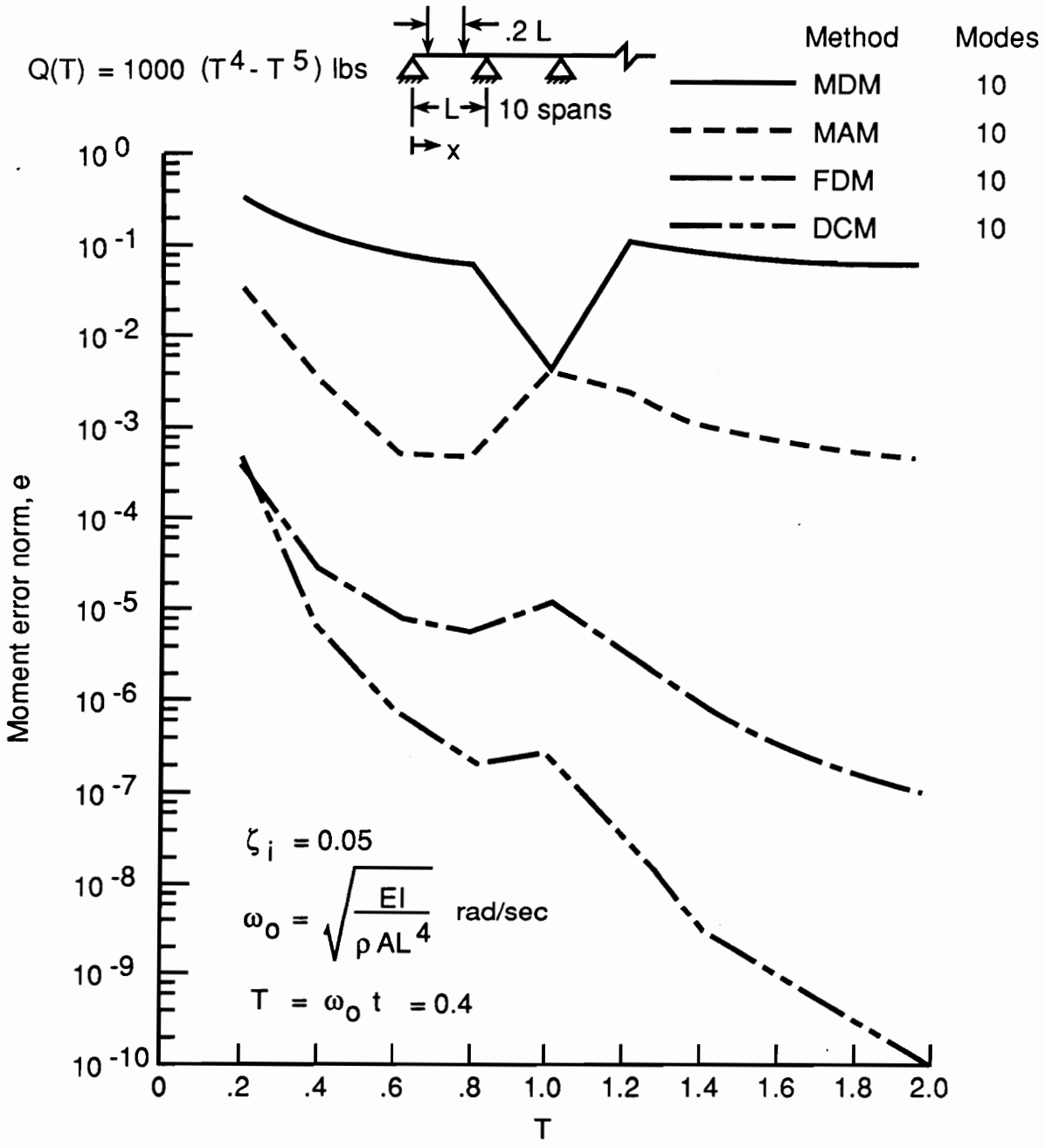

Figure 15. Variation of moment errors as a function of time, using 10 modes in the modal summation, for simply-supported multispan beam (ten equally-spaced spans) subject to two concentrated loads spaced about the center of the first span and varying in time as $Q(T) = 1000(T^4 - T^5)$ lbs., where damping ratios $\zeta_i = 0.05$.

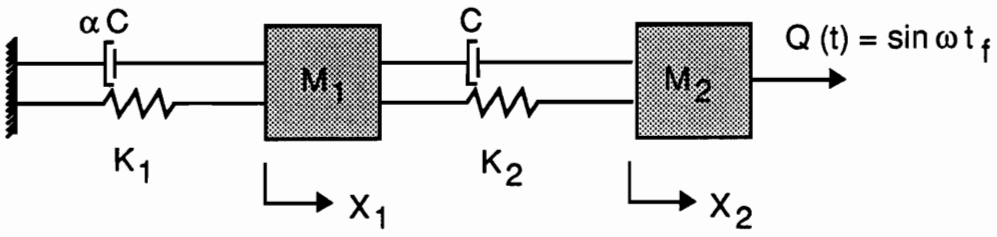

$M_1 = M_2 = 1$ Kg

$K_1 = K_2 = 1000$ N/mm

$C = 1$ N-sec/mm

$\alpha = 1$ - Proportional damping

$\alpha \neq 1$ - Non-proportional damping

Figure 16. Two-degree-of-freedom spring-mass-damper system.

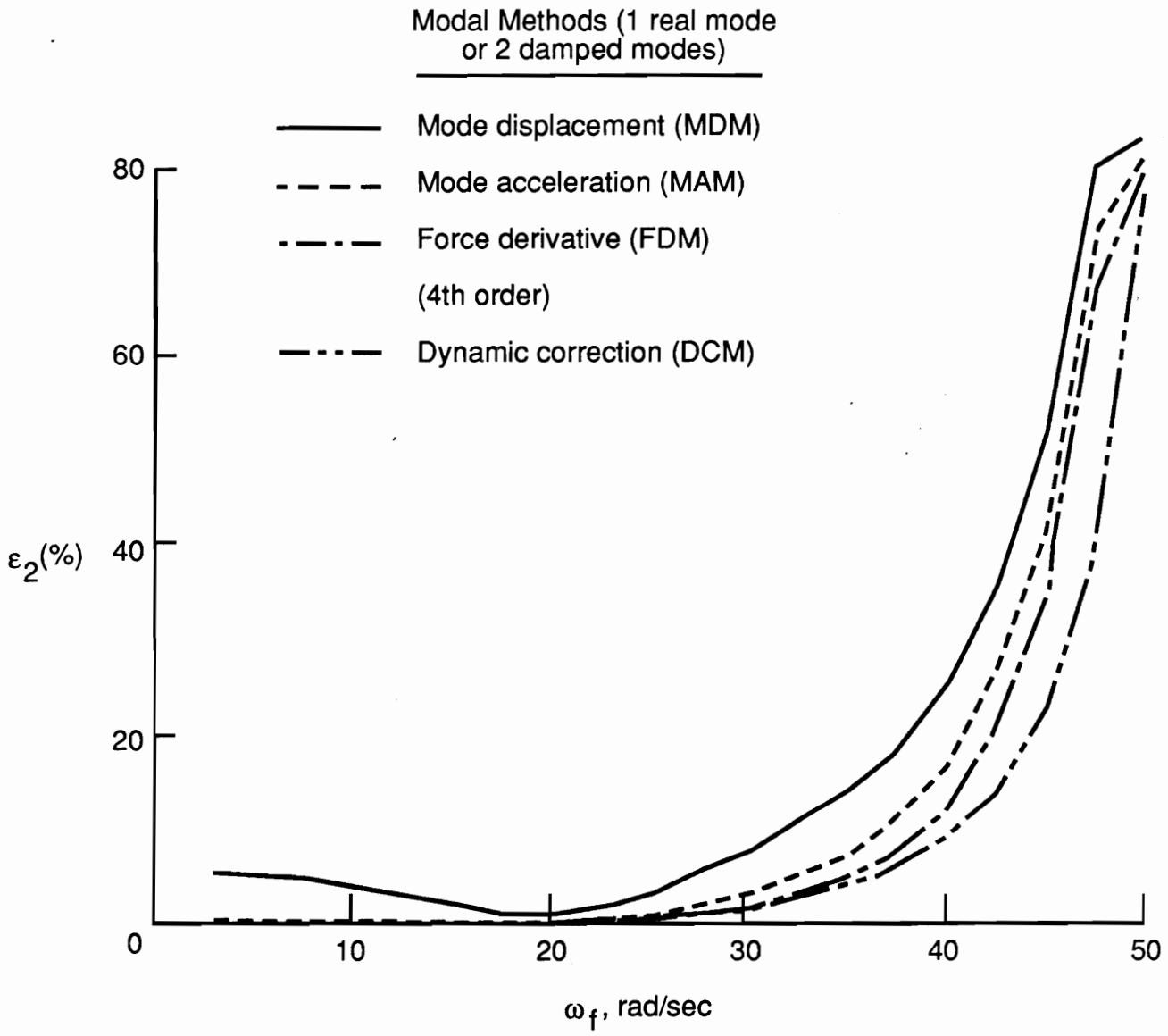

Figure 17. Comparison of various modal methods as a function of forcing frequency for a proportionally-damped two-degree-of-freedom problem where $\alpha = 1$.

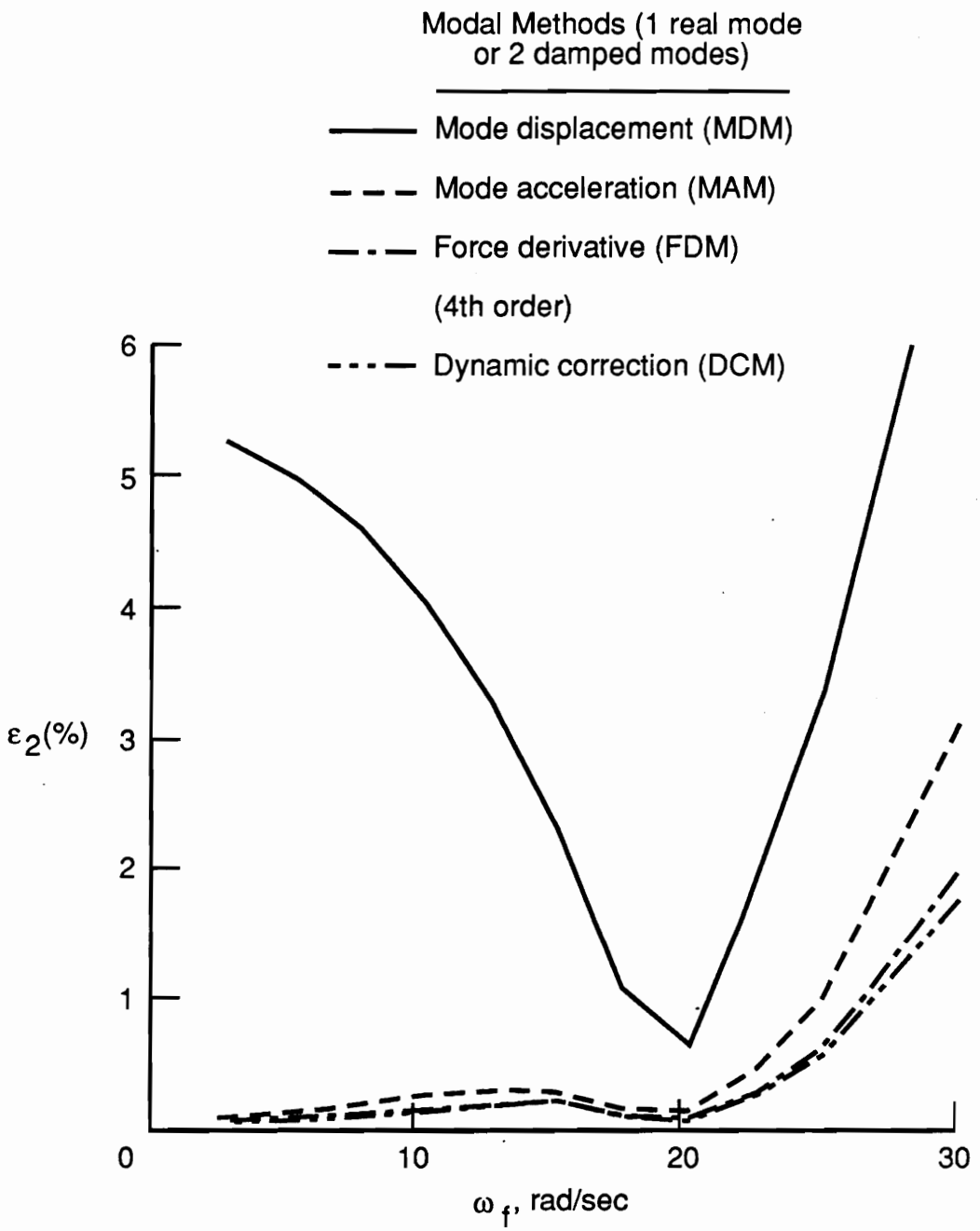

Figure 18. Comparison of various modal methods as a function of forcing frequency for a proportionally-damped two-degree-of-freedom problem where $\alpha = 1$.

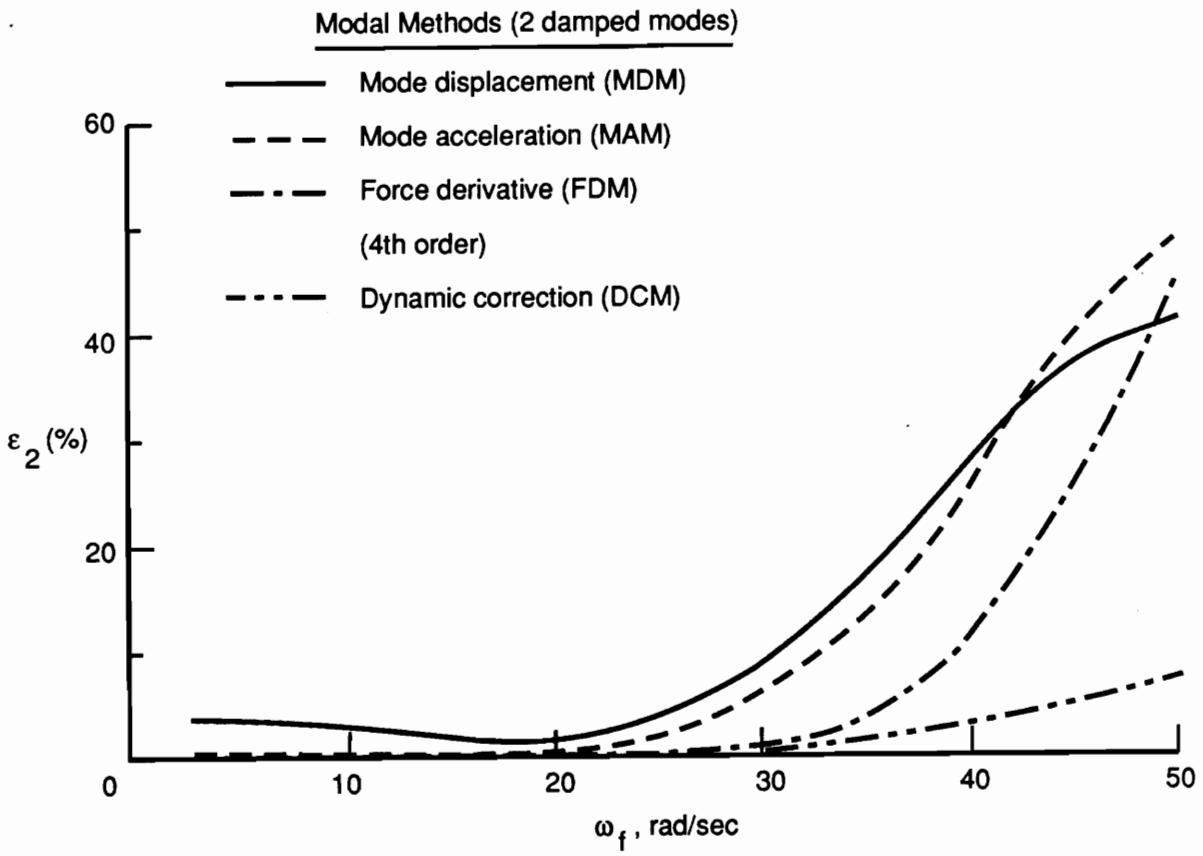

Figure 19. Comparison of various modal methods as a function of forcing frequency for a non-proportionally-damped two-degree-of-freedom problem where $\alpha = 20$.

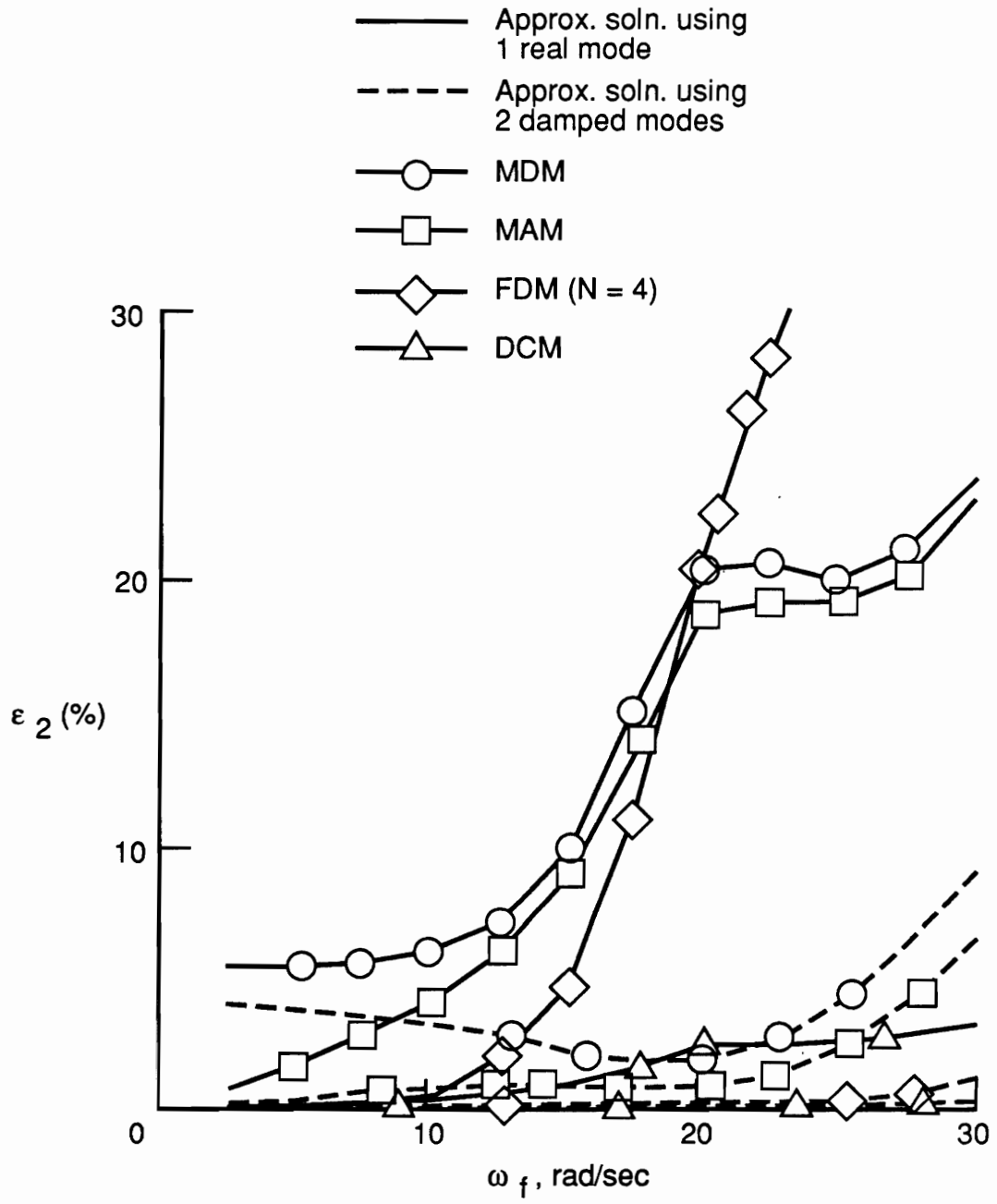

Figure 20. Comparison of damped- and natural-mode solutions for a non-proportionally-damped two-degree-of-freedom problem where $\alpha = 20$.

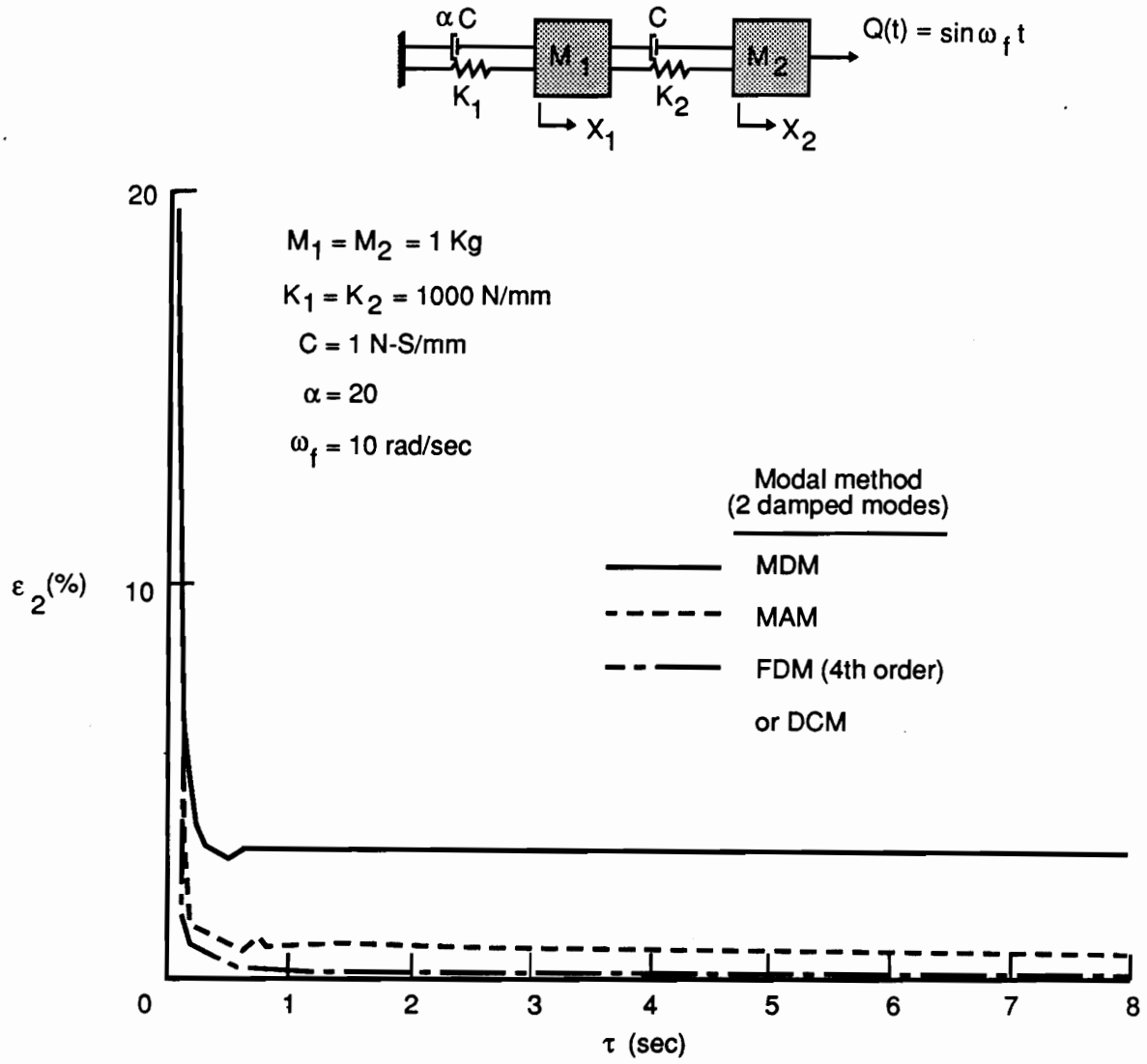

Figure 21. Comparison of various modal methods as a function of time for a non-proportionally-damped two-degree-of-freedom problem where α = 20. and ω_f = 10. rad/sec.

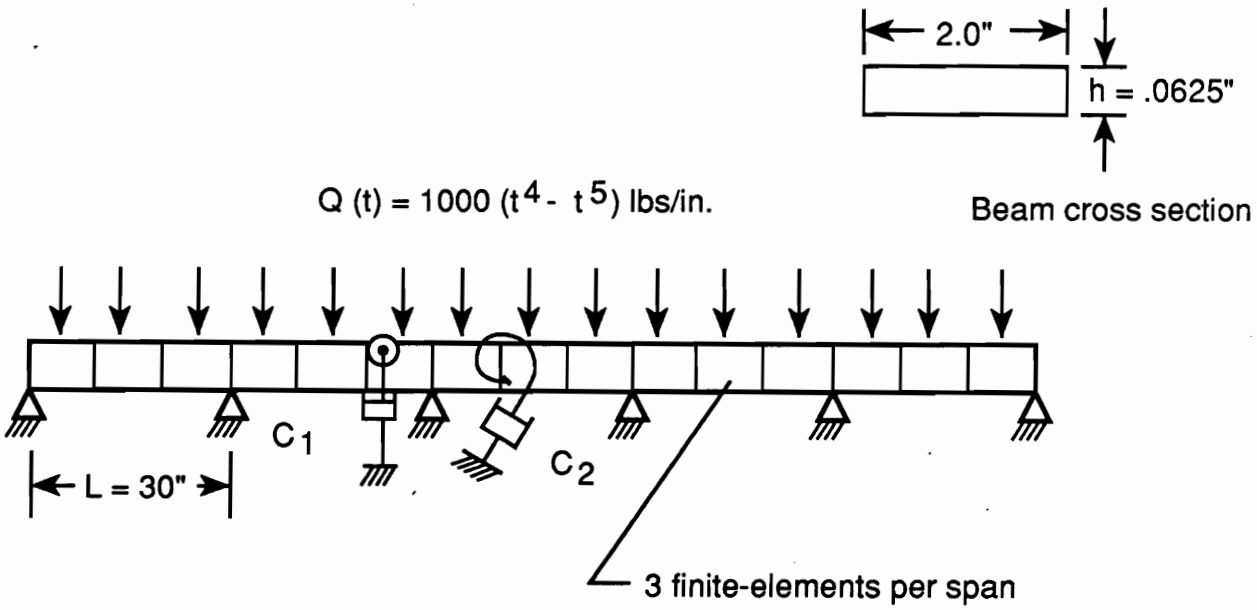

5-span beam

$E = 10 \times 10^5 lbs/in.^2$

$\rho = .28\ lbs/in.^3$

$C_1 = .008$ sec - lbs/in.

and

$C_2 = 1.2$ sec - lbs

} or $\xi_i = 0.05$

Material properties

Figure 22. Five-span beam with applied uniform, quintic time-varying load, $Q(T) = 1000(T^4 - T^5)$ lbs./in., and discrete dampers.

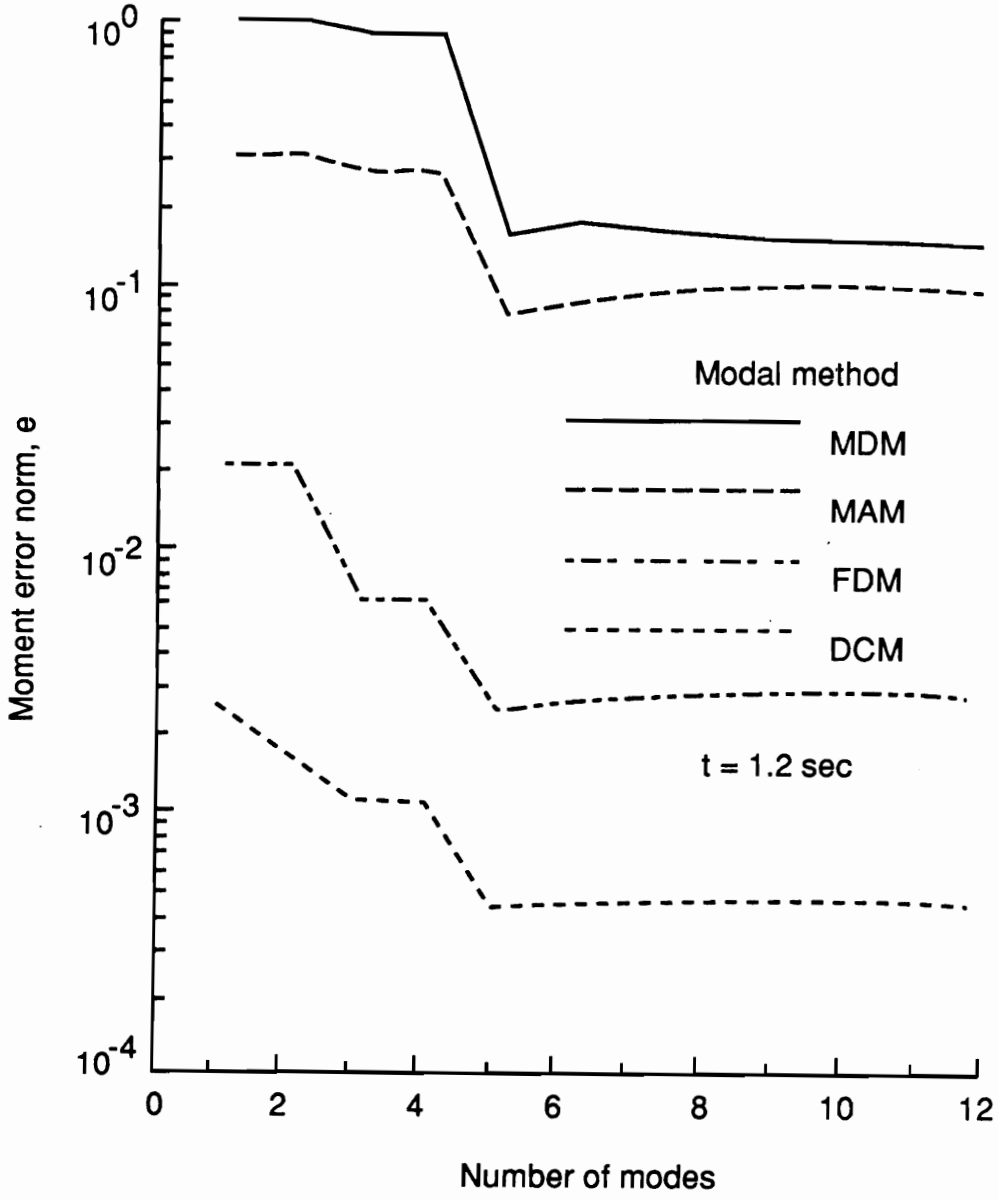

Figure 23. Comparison of moment errors of a simply-supported multispan beam (five equally-spaced spans) subject to a uniformly-distributed load varying with time as $Q(T) = 1000(T^4 - T^5)$ lbs./in., at $T = 1.2$ and with discrete damping.

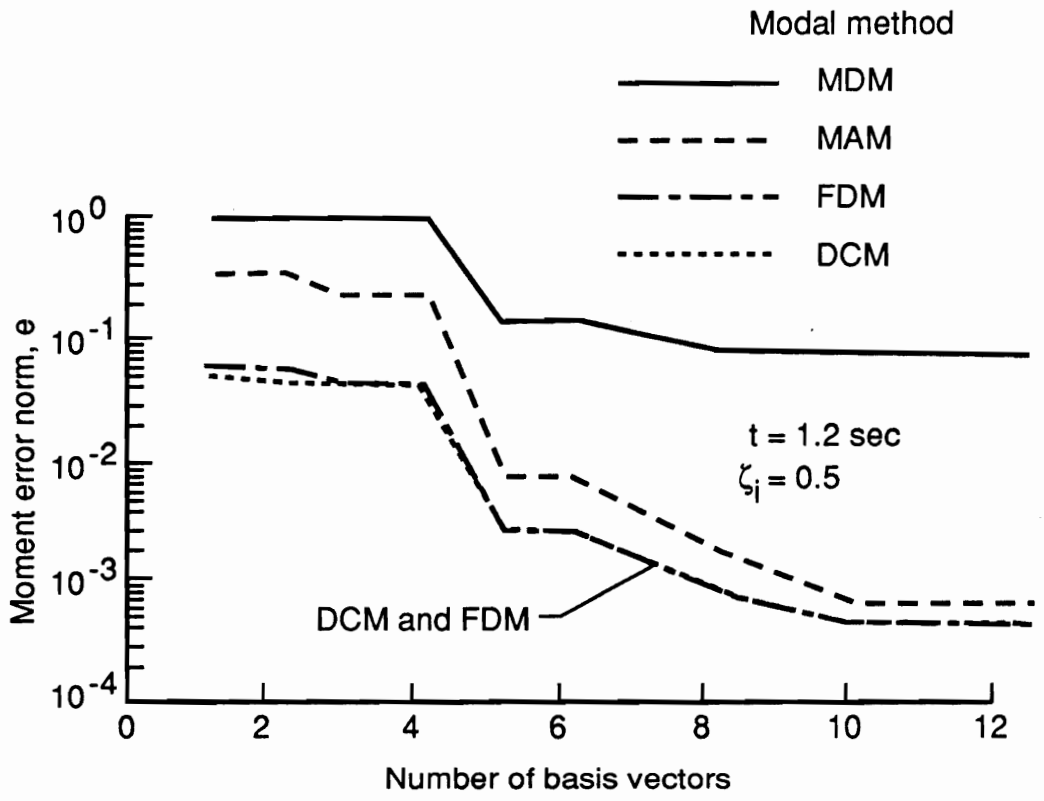

Figure 24. Comparison of moment errors of a simply-supported multispan beam (five equally-spaced spans) subject to a uniformly-distributed load varying with time as $Q(T) = 1000(T^4 - T^5)$ lbs./in., where $T = 1.2$ and proportional damping with damping ratios $\zeta_i = 0.05$.

Chapter 5

Thermal Analysis

Previous attempts at using mode superposition methods to solve transient, linear thermal problems (refs. 31 to 35) have been unsuccessful. Thermal problems typically exhibit a wide spectrum response where very high frequencies are excited and, hence, a prohibitively large number of "thermal modes" are necessary for an accurate solution. Results of references 32 and 33 indicate that Lanczos vectors can be effective reduced basis vectors for solving linear and non-linear transient thermal problems. Since the accuracy of the Lanczos vectors is comparable to that of the MAM for structural dynamic problems, it was expected that higher-order methods, such as the MAM, FDM, and DCM, would be effective in solving complex thermal problems also.

Higher-order modal methods, developed in Chapter 3 are used to solve a simple linear, transient heat transfer problem of a rod heated at one end.

The higher-order methods will be shown to be effective in significantly reducing the number of modes necessary to represent an accurate response.

5.1 Rod Heated at One End

The thermal problem selected to study is similar to that presented in reference 32. The rod is heated at one end and the temperature at the opposite end is constrained to zero (see fig. 25). The forcing function is a ramp heat load at one end which ramps up from zero to a peak value at time t = 10 sec and down to zero at time t = 20 sec as is shown in figure 25. The value of temperature at the unheated end is constrained to 0. The spacial error norm (eq. 45) is used to evaluate each of the modal methods.

A total of twenty equally-spaced finite elements were used to model the problem. Temperature distributions in the rod, calculated using the MDM, are shown in figure 26a. The exact solution, using all 20 degrees-of-freedom or modes, is illustrated by the solid line. At time t = 10 sec, the peak value of temperature is 400 at x/L = 0. An approximate solution using only 5 thermal modes underpredicts the peak value by 50 percent (T_{max} = 200) and results in unrealistic oscillations in the temperature distribution. If 10 and 15 modes are used, peak temperatures are underpredicted by 25 and 12 percent respectively. This error illustrates the inadequacy of the MDM in accurately predicting transient temperatures using a reduced set of "thermal modes". Temperature

distributions, calculated using the MAM, are shown in figure 26b. The MAM overpredicts maximum temperatures by over 25 percent when four modes are used in the solution. Once again, the temperature distribution oscillates, as shown by the dashed line, when an insufficient number of modes are used in the solution. The MAM requires approximately eight modes for a reasonable solution to this problem. The FDM also displays oscillations in the temperature distribution when an insufficient number of modes is used in the solution, however, results converge to an accurate solution using only five modes (fig. 26c). The effectiveness of using higher-order modal methods for reducing the size and computational effort of thermal problems is illustrated in figure 27. The FDM or DCM require about 28 percent of the number of modes as compared to the MDM and about 63 percent of the number of modes as the MAM for an accurate thermal response. The ability of the higher-order modal methods in predicting the transient thermal response accurately using very few degrees of freedom or modes, highlights the potential usefulness of these methods in reducing the computational size and effort in solving transient thermal problems.

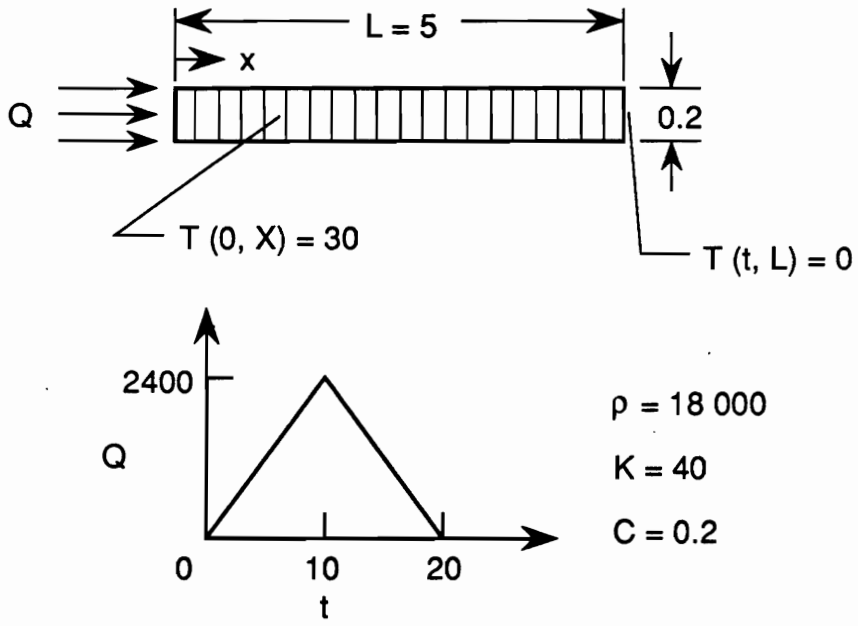

$$e = \sqrt{\frac{(T - T^a)^T (T - T^a)}{T^T T}}$$

Spatial error norm

where T^a = approximate temperature vector

Figure 25. One-dimensional heat conduction problem: rod heated at one end.

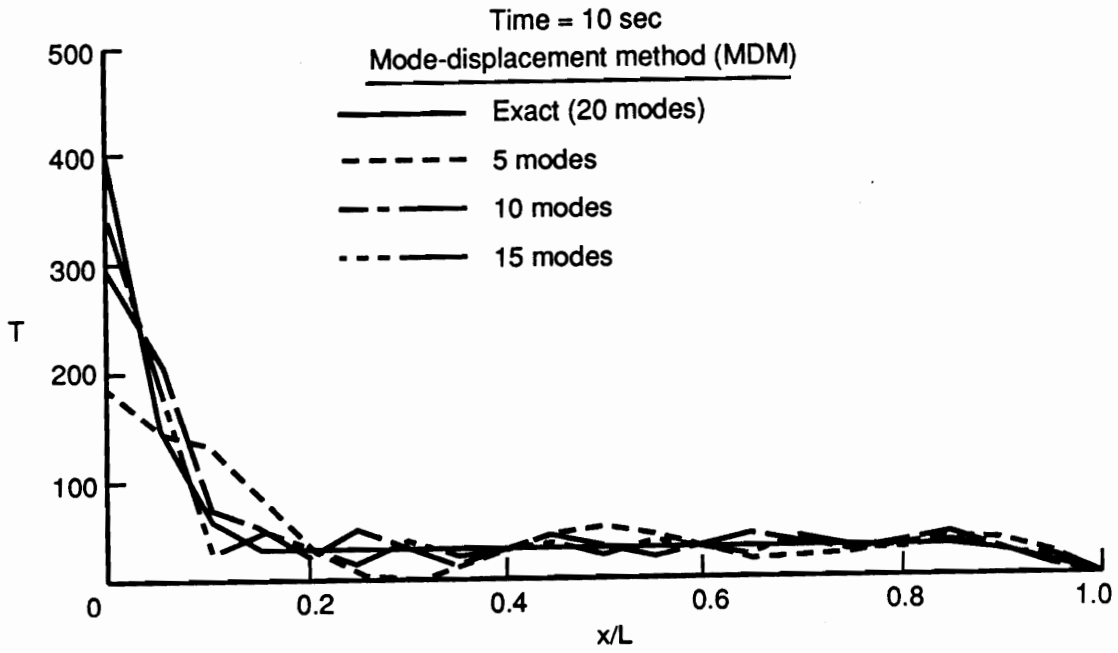

a) Mode-displacement method (MDM)

Figure 26. Temperature distribution along a rod heated at one end at time t = 10 sec.

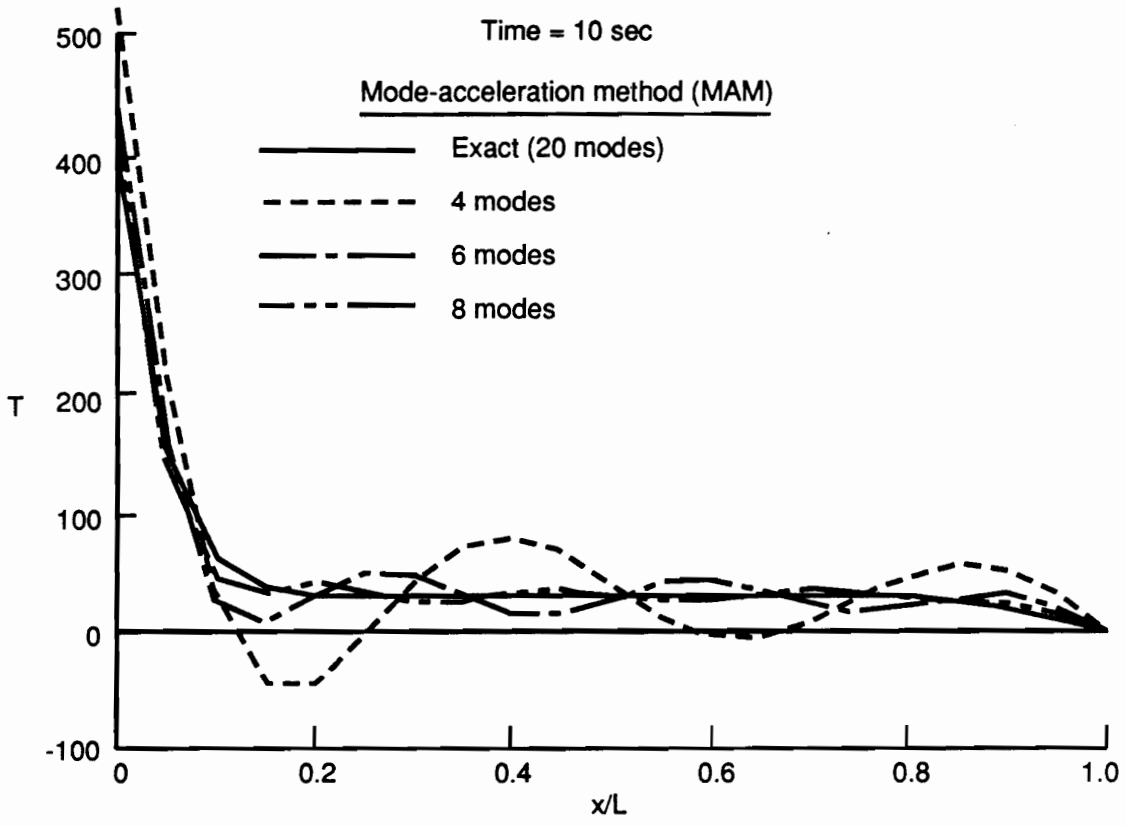

b) Mode-acceleration method (MAM)

Figure 26. Continued.

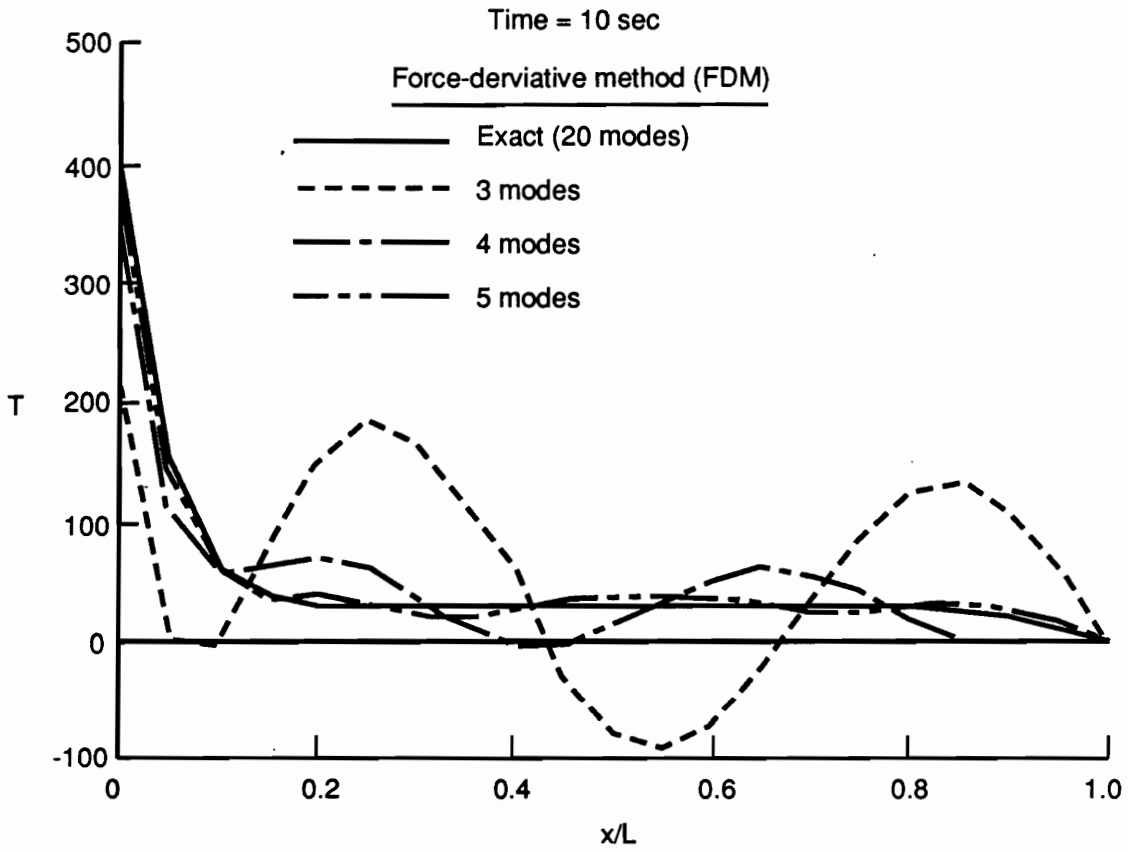

c) Force derivative method (FDM) and dynamic correction method (DCM)

Figure 26. Concluded.

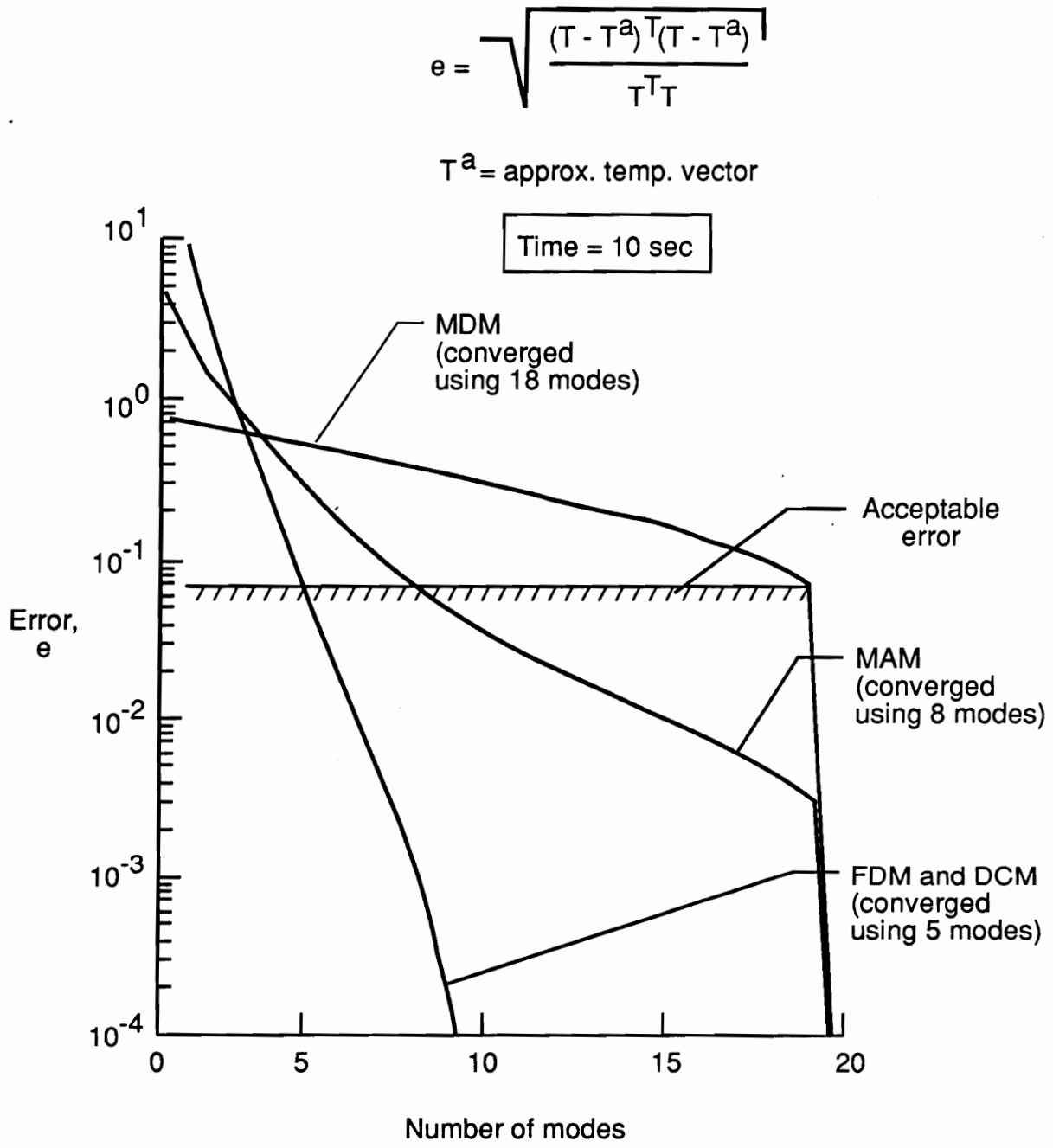

Figure 27. Convergence of modal methods for a one-dimensional, transient thermal problem at t = 10. sec.

Chapter 6

Concluding Remarks

A unified means for creating higher-order modal methods is presented which results in algorithms that have increased accuracy when solving transient, linear, thermal and structural problems. This new method is called the force-derivative method (FDM) because it is based on terms which are functions of the forcing function and its time derivatives. Several variations are presented for deriving the FDM for both a first-order system of equations and a second-order system. One representation results in expressions for either a first- or second-order system, which are well suited for inclusion into existing finite-element computer programs. The FDM unifies previously presented, lower-order methods such as the familiar mode-displacement method (MDM) and mode-acceleration method (MAM) of structural dynamics and is shown to be equivalent to another mode summation method, the dynamic-correction method (DCM), under certain conditions. In addition to structural dynamics, it is shown that the higher-order modal methods can be used to effectively reduce the size of

transient, linear thermal problems, where previous attempts, using the MDM, were fruitless. Approximate methods, such as the reduced basis methods, which are highly desirable for several reasons: they can drastically reduce the problem size and, hence, storage requirements and enable the solution of very large problems; and they can decrease the computational time and enable large optimization problems to become tractable.

These newly developed higher-order methods have been evaluated solely on the basis of their ability to decrease the number of degrees-of-freedom necessary to achieve a desired or predetermined accuracy. Accuracy has been determined quantitatively, using spatial and time-integrated error norms. The accuracy/convergence histories of various modal methods are compared for both uncoupled (proportionally-damped) structural problems as well as thermal problems and coupled (non-proportionally-damped) structural problems. The example problems which assume proportional damping include: a cantilevered beam subjected to a quintic, time-varying tip load and a step tip load and a multispan beam subjected to both uniform and discretely-applied quintic time-varying loads. Examples of problems with non-proportional damping include: a simple two-degree-of-freedom spring-mass system with discrete viscous dampers subjected to a sinusoidally-varying load and a multispan beam with discrete viscous dampers subjected to a uniformily-distributed, quintic time-varying load. The thermal example problem is a rod subjected to a linearly-varying tip heat load at one end with a constrained constant temperature at the opposite end.

The example problems were chosen to evaluate the effect of: 1) spatially and temporally discontinuous forcing functions, 2) forcing functions with vanishing higher derivatives, 3) discrete (non-proportional) damping and uniform proportional damping in all modes, 4) using "damped" or first-order eigenmodes compared to using "undamped" or second-order formulation, 5) the level of viscous damping, 6) closely-spaced frequencies (which occur in the case of repeated structural elements such as the multispan beam example), and 7) using higher-order modal methods in solving transient thermal problems.

In general, the FDM was found to be more accurate than either the MDM (zeroth-order method) or the MAM (first- order method) and results in a converged solution using fewer modes. The FDM, assuming an order of four, was less accurate than the DCM which is shown to be equivalent to the FDM under certain circumstance. The DCM, however, assumes a particular solution for the transient portion of the solution exists. For problems in which there are a large number of closely-spaced frequencies (e.g., large truss-type structures and multispan beams), the FDM is very effective in representing the effect of the important, but otherwise neglected, higher modes. Results for a multispan beam (10 equally-spaced spans) and a uniform, quintic time-varying load indicate the FDM and DCM methods both produce accurate results using only one mode as opposed to the MDM which required 49 modes and the MAM which required nine modes for similar values of error. The MDM and MAM results converge in a step-like manner with very little increase in accuracy as one to nine modes are used in the solution. This step-like convergence occurs because the first nine modes are orthogonal or nearly orthogonal to the uniform

loading distribution and hence produce a negligible modal load. For the case of discretely applied loads, the convergence is not step-like; however, the FDM and DCM methods still converge using many fewer modes than the MDM or MAM methods. More modes are required for convergence of the shear forces in the beam than for moment convergence and more modes are required for accurate moment predictions as compared to displacements. This is to be expected since the stresses are functions of the spatial derivatives of the displacements and the process of differentiation tends to magnify errors already existing in the displacement calculations.

At response times close to discontinuities in the forcing function and/or its derivatives, the MDM gives qualitatively better results than the higher-order methods, when few modes are used in the approximation. However when a sufficient number of modes are used to represent the discontinuity, the higher-order methods produce accurate results using fewer degrees of freedom. Implementation of the FDM or other higher-order methods requires the inclusion of appropriate jump conditions at the times discontinuities occur. It was also found that increasing the modal damping levels does not always increase the convergence rate of the MAM or other higher-order methods as was previously thought.

A first-order or "damped mode" solution was found to be effective in solving a non-proportionally damped two-degree-of-freedom problem. Results of this two-degree-of-freedom spring-mass-damper system subject to a sinusoidal forcing function indicate that, for the proportionally damped case, a solution using the first-order or "damped" form of the equations and two damped modes produces identical results as the second-

order or "undamped" form using one natural mode. Hence, there is no advantage in using a damped or first-order form to solve a proportionally-damped problem. However, for the non-proportionally damped problem, the use of two damped modes produces more accurate results than using only one mode and the second-order form. The DCM has the lowest percentage error of all the mode-superposition methods over the frequency range of 2 to 50 rad/sec. The FDM produced similar results to the DCM up to a forcing frequency of about 35-40 rad/sec. For the proportionally damped problem, all the methods were inaccurate near a frequency of 50 rad/sec (close to the second natural frequency of the system). A multispan beam with discrete dampers (non-proportionally damped) was studied and the results of the study indicate that the FDM and DCM converge using only one mode as compared to 15 for the MDM and 5 for the MAM.

The higher-order modal methods, such as the FDM, were found to be very effective in solving a simple one-dimensional thermal problem of a rod heated at one end. Previously, modal methods have been inefficient in solving thermal problems because the nature of the problem requires the inclusion of almost all the modes for an accurate solution. The ability of the FDM to approximate the effects of the higher, but neglected, modes results in an accurate solution using only five modes, out of a total of twenty modes for the rod problem, as compared to the MDM which required 18 modes and the MAM which required eight modes for an accurate solution.

REFERENCES

[1] Guyan, R. J.: Reduction of Stiffness and Mass Matrices. AIAA Journal, Vol. 3, No. 2, 1965, p. 380.

[2] Irons, B. M.: Structural Eigenvalue Problem: Elimination of Unwanted Variables. AIAA Journal, Vol. 3, No. 2, 1965, pp. 961-962.

[3] Leung, A. Y.-T.: An Accurate Method of Dynamic Condensation in Structural Analysis. International Journal for Numerical Methods in Engineering, Vol. 12, 1978, pp. 1705-1715.

[4] Masri, S. F.; Miller, R. K.; Sassi, H.; and Caughey, T.K.: A Method for Reducing the Order of Nonlinear Dynamic Systems. Journal of Applied Mechanics, Vol. 51, June 1984, pp. 391-398.

[5] Ramsden, J. N. and Stoker, J. R.: Mass Condensation: A Semi-Automatic Method for Reducing the Size of Vibration Problems. International Journal for Numerical Methods in Engineering, Vol. 1, 1969, pp. 333-349.

[6] Paz, M.: Reduction of Eigenproblems Using Modified Dynamic Condensation. In: Reanalysis of Structural Dynamic Models; Proceedings of the Symposium, Anaheim, CA, Dec. 7-12, 1986 pp. 29-34.

[7] Miller, C. A.: Dynamic Reduction of Structural Models. Journal of the Structural Division ASCE, Vol. 106, Oct., 1980, pp. 2097-2108.

[8] Wilson, E. L.; Yuan, M.-W.; and Dickens, John M.: Dynamic Analysis by Direct Superposition of Ritz Vectors. Earthquake Engineering and Structural Dynamics, Vol. 10, pp. 813-821, 1982.

[9] de Veubeke, Fraeijs, B. M.; Geradin, M.; Huck, A.; and Hogge, M. A.: Structural Dynamics – Heat Conduction. International Center for Mechanical Sciences – Courses and Lectures, No. 26. Springer, New York, 1972.

[10] Williams, D.: Displacements of a Linear Elastic System Under a Given Transient Load – Part I. The Aeronautical Quarterly, Vol. 1, August 1949, pp. 123-136.

[11] Cornwell, R. R.; Craig, R. R., Jr.; and Johnson, C. P.: On The Application of the Mode-Acceleration Method to Structural Engineering Problems. Earthquake Engineering and Structural Dynamics, Vol. 11, 1983, pp. 679-688.

[12] Leung, Y. T.: Fast Response Method for Undamped Structures. Engineering Structures, Vol. 5, April 1983, pp 141-149.

[13] Camarda, C. J.; Haftka, R. T.; and Riley, M. F.: An Evaluation of Higher-Order Modal Methods for Calculating Transient Structural Response. Computers and Structures, Vol. 27, No. 1, 1987, pp. 89-101,.

[14] Kline, K. A.: Dynamic Analysis Using a Reduced Basis of Exact Modes and Ritz Vectors. AIAA Journal, Vol. 24, No.12, December 1986, pp. 2022-2029.

[15] Leger, P.: Load Dependent Subspace Reduction Methods for Structural Dynamic Computations. Computers and Structures, Vol. 29, No. 6, 1988, pp. 993-999.

[16] Bushard, L. B.: On the Value of Guyan Reduction in Dynamic Thermal Problems. Computers and Structures, Vol. 13, 1981, pp. 525-531.

[17] Meirovitch, L.: Analytical Methods in Vibrations. The MacMillan Company, New York, 1967.

[18] Biot, M. A. and Bisplinghoff, R. L.: Dynamic Loads on Airplane Structures During Landing. NACA Wartime Report W-92, October, 1944.

[19] Nour-Omid, B. and Clough, R. W.: Dynamic Analysis of Structures Using Lanczos Co-ordinates. Earthquake Engineering and Structural Dynamics, Vol. 12, 1984, pp. 565-577.

[20] Tadikonda, S. S. K. and Baruh, H.: Gibbs Phenomenon in Structural Mechanics. Proceedings of AIAA/ASME/ASCE/AHS/ASC 30th Structures, Structural Dynamics and Materials Conference, Mobile, Alabama, April 3-5, 1989, Part 1, pp. 337-347.

[21] Haftka, R. T. and Kamat, M. P.: Elements of Structural Optimization. Martinus Nijhoff Publishers, Dordrecht, Netherlands, 1985, pp. 172-173.

[22] Sandridge, C. A. and Haftka, R. T.: Effect of Modal Truncation on Derivatives of Closed-Loop Damping Ratios in Optimal Structural Control. Journal of Guidance, Control, and Dynamics, Vol. 12, No. 6, Nov.-Dec., 1989, pp. 822-829.

[23] Greene, W. H., and Haftka, R. T.: Computational Aspects of Sensitivity Calculations in Transient Structural Analysis. Computers and Structures, Vol. 32, No. 2, 1989, pp. 433-443.

[24] Maddox, N. R.: On the Number of Modes Necessary for Accurate Response and Resulting Forces in Dynamic Analyses. Journal of Applied Mechanics, ASME, Vol. 42, 1975, pp. 516-517.

[25] Williams, D. and Jones, R.P.N.: Dynamic Loads in Aeroplanes Under Given Impulsive Loads with Particular Reference to Landing and Gust Loads on a Large Flying Boat. R & M No. 2221, Aeronautical Research Council Technical Report, London, England,1948.

[26] Rayleigh, J. W. S.: The Theory of Sound (Volume I). Dover, New York, 1945.

[27] Craig , R. R., Jr.: Structural Dynamics- An Introduction to Computer Methods. Wiley, New York, 1981.

[28] Hansteen, O. E. and Bell, K.: On the Accuracy of Mode Superposition Analysis in Structural Dynamics. Earthquake Engineering and Structural Dynamics, Vol. 7, 1979, pp. 405-411.

[29] Anagnostopoulos, S. A.: Wave and Earthquake Response of Offshore Structures: Evaluation of Modal Solutions. Journal of the Structural Division, ASCE, Vol. 108, No. ST10, October, 1982, pp. 2175-2191.

[30] Leger, P. and Wilson, E. L.: Modal Summation Methods for Structural Dynamic Computations. Earthquake Engineering and Structural Dynamics, Vol. 16, 1988, pp. 23-27.

[31] Gallagher, R. H. and Mallett, R.: Efficient Solution Processes for Finite Element Analysis of Transient Heat Conduction. ASME Winter Annual Meeting, Los Angeles, CA, 1969.

[32] Nour-Omid, B. and Wilson, E. L.: A New Algorithm for Heat Conduction Analysis. Numerical Methods in Thermal Problems (Part I), R. W. Lewis and K. Morgan editors, Pineridge Press, 1985, pp 18-29.

[33] Cardona, A. and Idelsohn, S.: Solution of Non-Linear Thermal Transient Problems by a Reduction Method. International Journal for Numerical Methods in Engineering, Vol. 23, 1986, pp. 1023-1042.

[34] Shore, C. P.: Reduction Method for Thermal Analysis of Complex Aerospace Structures. NASA TP 2373, January 1985.

[35] Coutinho, A. L. G. A.; Landau, L.; Wrobel, L. C.; and Ebecken, N. F. F.: Modal Solution of Transient Heat Conduction Utilizing Lanczos Algorithm. International Journal for Numerical Methods in Engineering, Vol. 28, 1989, pp. 13-25.

[36] Biot, M. A.: New Methods in Heat Flow Analysis With Application to Flight Structures. Journal of the Aeronautical Sciences, Vol. 24, No. 12, December, 1957, pp. 857-873.

[37] Ramberg, W.: Transient Vibration in an Airplane Wing Obtained by Several Methods. Journal of Research of the National Bureau of Standards, Research Paper RP1984, Vol. 42, May 1949.

[38] Likhoded, A. I.: Convergence of the Method of Expansion in Natural Vibration Modes in Programs of Dynamic Loading. Izv. AN SSSR. Mekhanika Tverdogo Tela, Vol. 21, No. 1, 1986, pp. 180-188.

[39] Borino, G. and Muscolino, G.: Mode-Superposition Methods in Dynamic Analysis of Classically and Non-Classically Damped Linear Systems. Earthquake Engineering and Structural Dynamics, Vol. 14, 1986, pp. 705-717.

[40] Camarda, C. J. and Haftka, R. T.: Development of Higher-Order Modal Methods for Transient Thermal and Structural Analysis. NASA TM 101548, February, 1989.

[41] Darnley, E. R.: The Transverse Vibration of Beams and the Whirling of Shafts Supported at Intermediate Points. Philosophical Magazine, Vol. 41, 1921, pp. 81-96.

[42] Warburton, G. B. and Soni, S. R.: Errors in Response Calculations for Non-Classically Damped Structures. Earthquake Engineering and Structural Dynamics, Vol. 5, pp. 365-676, 1977.

Vita

Charles J. Camarda was born May 8, 1952 in Queens, New York. He graduated from Archbishop John J. Molloy High School in Queens in 1970. He attended the Polytechnic Institute of Brooklyn where he graduated with a Bachelor of Science degree in Aeronautical Engineering in 1974. Upon graduation he began work at the NASA Langley Research Center in Hampton, Virginia. While working at NASA he participated in the George Washington University graduate program and received a Master of Science degree in Mechanical Engineering in 1980. Charles spent the 1983 academic year at the Virginia Polytechnic and State University working toward his Ph.D degree. Charles has one daughter, Chelsea Elise, and continues to work for NASA and reside in Virginia Beach.

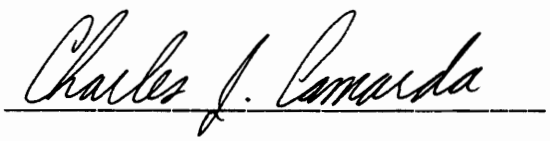

Charles J. Camarda